# Retrieval of Solvent Injected During Heavy-Oil Recovery in Heterogeneous Porous Media: Pore Scale Analysis through Micro Model Experiments

by

Jingwen Cui

A thesis submitted in partial fulfillment of the requirements for the degree of

Master of Science

in

Petroleum Engineering

Department of Civil and Environmental Engineering
University of Alberta

# Abstract

Solvent retrieval is essential for the economics of the solvent-related heavy-oil recovery technologies. In fractured and oil-wet reservoirs, water-flooding followed by solvent is not suitable to achieve this goal. Two methods can be proposed as solution to solvent retrieval in complex reservoirs: (1) Thermal: Hot water or steam injection to vaporize the solvent; (2) Chemical: Addition of surface active agents to alter wettability for effective matrix-fracture transfer.

This thesis aimed to investigate the mechanics of these two methods at the pore-scale. A series of experiments using heterogeneous micro-models were designed for this purpose. The process of solvent vaporization and entrapment during heating followed by solvent injection was evaluated using the images obtained from the experiments. Evaluations were made using the parameters (pore size, wettability, interfacial tension, and solvent type) in the Thomson equation. The nucleation of solvent and the distribution of fluids/phases emerged through this process were qualitatively analyzed. Suitable application conditions (temperature, heating source location) for different solvent types and wettability were determined.

Next, selected chemicals (conventional surfactants and new generation –nano-chemicals) were tested as an alternative to solvent injection to recover heavy-oil and as a material to retrieve the solvent instead of applying heat injection methods. Proper chemical types were identified for effective solvent retrieval and heavy-oil recovery from different wettability conditions and solvent types.

## Acknowledgments

As I approach the end of my two-year study for master's degree, I started to realize how privileged I was having the opportunity to study here at the University of Alberta. I would like to express my deepest gratitude to my parents who always stand behind me and encourage me to do what I believe. I want to thank my supervisor, Dr. Tayfun Babadagli who gave me this valuable opportunity and provided continuous guidance, advice and support. I learned a lot from him through this journey over the last two years.

This research was conducted under Dr. Babadagli's NSERC Industrial Research Chair in Unconventional Oil Recovery (industrial partners are CNRL, SUNCOR, Touchstone Exp., Sherritt Oil, APEX Eng., Husky Energy, Saudi Aramco and PEMEX) and an NSERC Discovery Grant (No: G121210595). I gratefully acknowledge these supports.

I would like to express my special thanks to our laboratory assistants, Mihalea and Lixing, who provided endless help during my experiments with patience. I also am thankful to Pam Keegan who carefully edited my papers, and all others in the EOGRRC group members for their support and friendship.

Finally, I would like to thank my friends Daimeng, Xiaoxing and Jianyi, who were with me when I had any trouble. We shared the great moments of these two years together and saw each other's growth.

## Contents

# List of Tables

# List of Figures

# CHAPTER 1: INTRODUCTION

## 1.1 Background

Thermal methods are widely applied for heavy-oil recovery. The most common technique is steam based applications. The cost and efficiency, along with the environmental and operational problems, are restrictions to steam injection. As an alternative, sole-solvent injection or technologies combining solvent with thermal methods were proposed and investigated over the past years. The main concern in solvent applications is the efficient retrieval of it for economic viability.

In homogenous and light-oil reservoirs, simple water injection was proposed for this purpose and successful applications of WAG (water alternating gas) have been reported. But, in heterogeneous reservoirs composed of fractures or worm-holes with matrix containing great amount of oil, retrieving the solvent diffusion into it is problematic. Hot water or steam injection was proposed to vaporize and retrieve the solvent transferred into the matrix by Al-Bahlani and Babadagli (2008). Their newly patented SOS-FR (steam-over-solvent injection in fractured reservoirs) technology was tested by core-scale static and dynamic experiments and proved that the estimated recovery factor of the injected solvent is around 85-90% at the end of solvent-retrieval stage (Al-Bahlani and Babadagli 2008).

If the combination of solvent and thermal methods was found too expensive, waterflooding with wettability alteration additives can be considered an alternative. New generation wettability-alteration agents were tested by Mohammed and Babadagli (2016) through core scale experiments used in solvent retrieval and heavy-oil recovery from carbonates and sandstones. If suitable chemicals and application conditions are determined, this approach can be economically viable and become an alternative to solvent-thermal methods.

## 1.2 Statement of the Problem

Solvent injection has been tested for sole use or in combination with a thermal method to develop heavy oil or bitumen reservoirs. To retrieve the expensive solvent back, alternative injection of water or steam by viscous displacement could be applied in homogenous reservoirs. For the complex system such as fractured carbonates or solvent injection after CHOPS (cold heavy oil production with sands), the solvent diffused into less permeable matrix portion is more easily trapped and requires more efficient technology. The design of injecting hot water or steam to vaporize the solvent was proposed and tested in a series of research in the past.

Naderi and Babadagli (2013) applied the SOS-FR process on the cores of the Grosmont carbonates where recovery was controlled by heterogeneity and fracture network. During their experiments, the solvent retrieval phase was extremely quick and high (62%-82%) when they set the temperature of hot water at around 90°C. Due to heat loss in thin layered reservoirs, solvent aided steam technologies were also a focus to develop the large amount of oil unproduced after CHOPS recovery. Coskuner et al. (2013) applied the similar experimental procedure to understand the SOS-FR after CHOPS. While injecting hot water for solvent retrieval by vaporization at the end of the process, hot water vaporized the diffused solvent and then imbibed into the cores. It was calculated that 45%-55% of the solvent was recovered during the retrieval process.

The previous research made us question several important issues regarding solvent retrieval:

- How did the bubbles of solvent form, nucleate and mobilize from matrix to fracture? Did solvent get trapped in the matrix in the form of liquid or vapor?
- How was the phase distribution developed through this complex process in the pores of the matrix?

- How is the efficiency of solvent retrieval if chemical was applied to reduce interfacial tension or alter wettability?
- What are the ideal conditions to maximize the solvent retrieval?
- Can chemically augmented waterflooding be an alternative to heavy-oil recovery (no pre-solvent injection) or solvent retrieval (chemical injection after solvent diffusion)?

Marciales and Babadagli (2016) designed experiments using 2-D micromodels to answer some of these questions. They reported observations from six experiments in which heptane and naphta were used as solvents applying different heating at different conditions. Based on their initial trials reported in this work, we continued and focused not only on the solvent type but also oil viscosity and wettability of the system. More experimentation is needed to understand the applicability of the Thomson equation to heavy-oil containing porous media and clarify the temperature needed to boil the solvent for retrieval.

Micro-fluidic device was considered to be useful to also answer several questions as to the solvent entrapment and retrieval mechanisms if water was injected with chemical additives. Mohammed and Babadagli (2016) provided core scale experiments using many different chemicals. Although very promising and valuable data were obtained in this work, pore-scale visual experiments are still needed to clarify the wettability alteration mechanism and solvent entrapment and transfer into fractures from matrix when different chemicals are used.

## 1.3 Aims and Objectives

This research aims to perform the following objectives:

1. Design a 2-dimensional visualization set-up based on micromodel to simulate the solvent retrieval process;
2. Investigate the mechanics of the thermal methods to retrieve the solvent and observe the forming, development, and nucleation of the bubbles;
3. Discuss the effect of the following parameters on the solvent retrieval during the heating stage:
    - Solvent type
    - Oil type
    - Heating rate
    - Heating location
    - Wettability
4. Visualize the micro-emulsion phenomena and matrix-fracture interaction through wettability alteration during heavy-oil recovery without pre-solvent injection, and screen the following surfactant types and nano-fluids:
    - Sulfonate series
    - Nano-fluids
    - Ionic liquids
5. Visualize how chemical flooding can be applied when it is coupled with pre-solvent injection and heating.

Items 1, 2, and 3 are covered in Chapter 2 of this thesis. Chapter 3 contains the outcome of the research study on Items 4 and 5.

## 1.4 Structure of the Thesis

This is a paper-based thesis composed of four chapters. Chapter 1 introduces the background, a statement of the problem and research objectives. Then, two chapters are papers, which were prepared for a conference or submitted to a journal.

Chapter 2 presents the solvent retrieval process in 2-dimensional micro-model. The vaporization of the solvent played an important role; therefore, the related parameters such as heating location, heating rate, solvent type, oil viscosity, and wettability, which control the vaporization process, were controlled and compared. The formation, nucleation, and production of the solvent in gas phase under different conditions are presented. The effects on the two phase equilibrium caused by the porous media are also presented.

In Chapter 3, micromodel provided a visual method to screen the efficient chemical, which could enhance the sweep efficiency of the fractured system. The micro-emulsion and wettability-alteration phenomena in pore-scale are presented and compared. Then selected agents are applied to assist in the thermal process to maximize the amount of solvent retrieved.

In Chapter 5, the main contributions of this work are listed for future work.

## 1.5 References


Al-Bahlani, A.M. and Babadagli, T. 2008. Heavy-Oil Recovery in Naturally Fractured Reservoirs with Varying Wettability by Steam Solvent Co-Injection. Presented at the 2008 International Thermal Operations and Heavy Oil Symposium, Calgary, Alberta, Canada, 20-23 October. SPE-117626-MS. http://dx.doi.org/10.2118/117626-MS.

Coskuner, G. 2013, Naderi, K., and Babadagli, T. 2013. An Enhanced Oil Recovery Technology as a Follow Up to Cold Heavy Oil Production with Sand. Paper presented at the SPE Heavy Oil Conference-Canada, Calgary, Alberta, Canada, 11-13 June. SPE-165385-MS. http://dx.doi.org/10.2118/165385-MS.

Marciales, A. and Babadagli, T. 2016. Pore scale visual investigations on solvent retrieval during oil recovery at elevated temperatures: A Micromodel Study. *Chemical Engineering Research and Design* **106**: 59-73.

Mohammed, M. A., and Babadagli, T. 2016. Experimental Investigation of Wettability Alteration in Oil-Wet Reservoirs Containing Heavy Oil. *Journal of SPE Reservoir Evaluation & Engineering*. Preprint (to appear). SPE-170034-PA. http://dx.doi.org/10.2118/170034-PA.

Naderi, K., Babadagli, T. and Coskuner, G. 2013. Bitumen Recovery by the SOS-FR( Steam-Over- Solvent Injection in Fractured Reservoirs) Method: An Experimental Study on Grosmont Carbonates. Paper presented at the SPE Heavy Oil Conference-Canada, Calgary, Alberta, Canada, 11-13 June. SPE-165530-MS. http://dx.doi.org/10.2118/165530-MS.

# CHAPTER 2: Retrieval of Solvent Injected During Heavy-Oil Recovery from Water- and Oil-Wet Reservoirs: Pore Scale Analysis at Variable Temperature Conditions

A version of this chapter was presented and published at SPE Latin America and Caribbean Heavy and Extra Heavy Oil Conference held in Lima, Peru, 19–20 October 2016 (SPE Paper 181166). It has also been submitted to a journal for publication.

## 2.1 Preface

To make the solvent EOR processes efficient, retrieval of expensive solvent efficiently is required. In case of heterogeneous reservoirs (fractured carbonates or sands with wormholes), one needs to develop techniques other than viscous displacement to retrieve the solvent diffused into less permeable matrix portion. Previous core-scale experiments have provided valuable data to optimize this process, but the mechanics of the nucleation of the solvent vapor and its entrapment in the pores at the micro scale under variable temperature conditions requires further research.

A series of experiments using a 2-D etched glass micromodel (sandstone replica with a fracture) were carried out to investigate the mechanics of solvent retrieval and entrapment. The micromodel was saturated with dyed processed oil and different solvents were injected through fracture. After the solvent was diffused into matrix completely to recover the oil, the model was heated mimicking a thermal method to reach the boiling point of the solvent and retrieve it. Different parameters such as wettability, heating rate, and pore-scale fluid composition were controlled and compared during the heating phase. Finally, water was injected to retrieve the remaining solvent in the liquid or vapor phase.

Visual observations of solvent diffusion/dispersion into matrix and its retrieval from the matrix clarified the miscibility process in the presence of an immiscible phase, interaction between different phases in a complex heterogeneous system, and phase distributions as a function of temperature.

## 2.2 Introduction

Thermal processes are widely applied to develop heavy oil and bitumen reservoirs, mainly aiming to reduce the viscosity of oil. These processes may not be efficient due to heat loss in thin layers, bottom-water reservoirs and heterogeneous carbonates. The use of solvent in thermal applications to improve the efficiency of the process and to further reduce oil viscosity has been considered recently. Co-injection of solvents with steam or pre-injection of them before starting steam injection processes were tested extensively (Ali and Abad 1976; Redford and Mckays 1980; Shu and Hartman 1988; Nasr et al. 2003, 2005, 2006). Solvent was also designed to inject alternately with steam (Zhao et al. 2004, 2005). Recovering very viscous oil through injecting superheated solvents was patented by Aleen et al. (1984). The solvent performance during thermal applications is highly dependent on temperature. Pathak et al. (2010, 2011) showed a remarkable variation of recovery with an increase in temperature for the hot solvent injection process. Steam-over-solvent injection (SOS-FR) method was proposed specifically for naturally fractured (oil-wet) reservoirs (Al-Bahlani and Babadagli 2009; Babadagli and Al-Bahlani 2008). Later, experiments and numerical simulations were conducted to help find and design optimum solvent type, concentration and operating parameters to achieve these technologies (Govind et al. 2008, Li and Mamora 2011; Leyva-Gomez and Babadagli 2015).

Injected solvent is a much more expensive substance than the produced heavy oil or bitumen. To make solvent-aided heavy-oil recovery processes efficient, the retrieval of solvent injected at acceptable rates is essential for the operability and economics of these technologies. Gupta et al. (2004) investigated capillary adsorption which could cause solvent retention in porous media and analyzed the importance of recycling solvents when discussing the economics of solvent aided

steam injection process. Chang et al. (2013) investigated different mechanisms involved in solvent retention behaviour in porous media.

In light oil and homogeneous reservoirs, water injection is able to sweep residual solvent. In heterogeneous systems like fractured carbonate reservoirs, the oil is stored in the matrix but the fracture controls the flow. The method of water injection may not be efficient and making use of solvent vaporization at higher temperature was proposed for this kind situation. Al-Bahlani and Babadagli (2008, 2009a) proposed a new technology (SOS-FR) to develop the heavy oil in fractured reservoirs efficiently. At the final step of the whole process, steam or hot water was injected to heat the residual solvent at around boiling point temperature of the solvent to retrieve it thermodynamically. Mohammed and Babadagli (2013) further tested the efficiency of solvent retrieval by heating the reservoir after completing the solvent injection phase. They designed a series of static core experiments to estimate the rate and ultimate amount of solvent retrieval by hot water injection and concluded that 86-90% of the solvent introduced into rock matrix was retrieved if an optimal temperature is applied. In their work, efforts were made to clarify the physics behind this process in core scale and identify the roles of the parameters such as wettability and temperature.

More efforts are needed to clarify the effect of critical parameters (solvent type, temperature, wettability, etc.) on the solvent retrieval process, especially at the pore scale with visual evidences. Marciales and Babadagli (2015) designed experiments using 2-D micromodels and vaporized the solvent diffused into porous media at elevated temperatures. They used heptane and naphta as solvent and achieved the retrieval of them by heating at different conditions. The present paper, in a sense, is a continuation of this work. Our focus is not only on the solvent type but also oil viscosity and the wettability of the system.

We visually analyzed the vaporization and mobilization of solvent under heating. The bubble nucleation and expansion in porous media was imaged for different conditions (i.e., heating source, temperature level, heating rate, rock wettability, and oil and solvent types).

## 2.3 Experimental Methodology and Procedure

A series of experiments were designed using a square-shaped Berea-sandstone-replica model made by etched glass following the procedure introduced by Naderi and Babadagli (2011). The depth of the channel was 40μm and all micromodels had a 5 cm × 5 cm matrix (porous part) and a 1 cm × 5 cm conduit to represent a fracture or wormhole. As the glass substrate is naturally water-wet, the micromodel is assumed to be initially water-wet.

An entry port and one production port were set at the opposite corners of the fracture side (**Fig. 2.1**). The visual window (the area marked by yellow square on the micromodel shown in Fig. 2.1) to capture images was fixed in the middle of the fracture for experimental comparison and also to reduce the edge effect. Proper dying agents were chosen and added to varying liquids differently: DFSB-K175 for oil, DFSB-K43 for solvent and IFWB-C8 for water from Risk Reactor (2014). Oil, matrix grains, and solvents were classified and shown as brown, black, and cyan under filtered UV light (**Fig. 2.2**). The miscible mixture of oil and solvent is shown as color between these two and marked in the images. The gas phase (bubbles) is identified by black color with white outline as shown in **Fig. 2.3**. The white line represents the interface between the gas phase and the liquid phase (or matrix grains).

A Canon 7D camera recorded the images during the experiments. Syringe pump was used to inject oil and solvent at low pressure. A heating plate was controlled to heat the certain part of the micromodel to retrieve the solvent. There were two thermocouples fixed on two testing

points (marked in Fig. 2.2) to monitor the continuous temperatures of the fracture and matrix. Temperatures were recorded every 5 min by thermocouples and a data acquisition system. The detailed set up is shown in Fig. 2.1.

Two kinds of mineral oils (250cp; 600cp at 25°C) were chosen to investigate the effect of oil viscosity. Heptane and decane were injected through the fracture to be miscible with the mineral oil in the matrix. Subsequently, the system was heated to vaporize the solvent. A chemical dichlorooctamethyltetrasiloxane (SurfaSil, a siliconizing liquid) was applied to micromodel before experiments to alter wettability to more water-wet (details of this process can be found in Naderi and Babadagli [2011]). The wettability alteration was validated by contact angle tests as well as through the observation of water/oil or water/solvent interfaces during experiments.

At the beginning of the experiment, the mineral oil was injected to fill the pores of the micromodel with it (Fig. 2.2). Then, solvent was injected at a low rate of 1ml/hr to occupy the whole fracture part. This procedure was applied for the lighter oil (250cp); but, for the heavier (600cp) oil, two options were designed. (1) Inject the solvent at 1ml/hr after around 10 hr to fill the fracture and let the solvent completely mixed with the mineral oil in the matrix until equilibrium. (2) Inject more solvent for 16 hr. The next step started until the solvent had sufficient time (almost 12 hr) to mix with oil in the matrix and reach equilibrium as indicated in Fig. 2.2.

Note that this part of work was performed to reach the miscible stage. It does not target at any enhanced oil recovery assessment or so. Therefore, excess amount of solvent was injected to fully reach miscibility. Then, the solvent retrieval process, which is the main goal of this research, was initiated and the micromodel was gradually heated by continuously increasing

temperature. The location of the heater (heating point) and the heating rate for each experiment are described in **Table 2.1**. Depending on the heating conditions, different boiling phenomena of solvent were observed. The detailed analysis of this process will be discussed later. The heating efficiency rate was adjusted by different heating time to reach the same final temperature. Considering the durability of the micromodel materials, the final temperature was fixed at 75°C and 100°C for heptane and decane, separately. Once these temperature values were reached, the heating source was shut down and the system was let down to cool to the ambient temperature.

The visualization study aimed to investigate how different parameters affect the solvent retrieval process, especially during the boiling process. The parameters tested are (1) heating boundary conditions (location of heater), (2) heating rate, (3) oil and solvent type, and (4) wettability. Then images were processed and in some cases converted to black and white with different gray tones. The values of phase saturation and microscopic recovery factor were determined by the area occupied by a certain phase when comparing to fixed observation area. The details of the experiments are shown in Table 2.1.

## 2.4 Results and Discussion

### 2.4.1 General Vaporization Process

After solvent diffused into the matrix, only fracture part of the micromodel was chosen to be heated in Experiment 1. When temperature of testing point was increased to 55°C, the first solvent bubble appeared near the bottom of the fracture as shown in **Fig. 2.4**. The bubbles gradually occupied the fracture and then invaded into the pores of the matrix as also illustrated in Fig. 2.4. These bubbles grew horizontally and vertically displacing the continuous (liquid) phase.

The close-up views in **Fig. 2.5** illustrate how the solvent were distributed during the solvent vaporizing process. The liquid solvent was trapped by gas bubbles as indicated in Fig. 2.5 (liquid solvent trapped marked by the red circle). The gas bubbles grew up further in matrix vertically and were connected with other bubbles as the orange circle pointed out.

**Fig. 2.6** shows how heating rate affected the solvent boiling process comparing three different heating strategies. Figs. 2.6a, 2.6e and 2.6i display the temperature profiles developed during the heating process. The orange and blue curves represent the temperature of matrix and fracture, respectively. As the whole micromodel was heated and temperature was uniformly distributed in Experiment 3, there was only one curve, as shown in Fig. 2.6i, to represent the temperature profile. Heating in Experiment 2 was slower than Experiment 1, which means it was more efficient; i.e., less heat energy was used per given time. The vertical growth of bubbles in Experiment 2 (marked by yellow line in Fig. 2.6h) was further than in Experiment 1 (indicated in Fig. 2.6d) at the same temperature.

### 2.4.2 Effect of Heating Location

Uniform heating was applied to the micro-model in Experiment 3 (the whole micromodel was heated uniformly and the temperature distribution turned out to be uniform throughout the model). There was no temperature gradient through the whole micro-model and only one testing point was set for recording temperature. As the required boiling temperature is lower in smaller pores, the solvent in the matrix started boiling earlier. It was observed that solvent bubbles quickly distributed in the whole micro-model as a continuous phase shown in Fig. 2.6l. As mentioned, strong heating boosted the vertical development of bubbles. At the same time, gas bubbles quickly bypassed the throats and smaller pores (red circled parts in **Fig. 2.7**). The

existence of bubbles showed a non-wetting behaviour (in the form of filaments with liquid solvent coating the walls of the pores) as indicated by as yellow squares in Fig.2.7. After analyzing the images of the final temperature, the percent of the matrix area occupied by the trapped liquid solvent were 16.8%, 0.09%, and 12% averagely in Figs. 2.6d, 2.6h and 2.6l. The retrieval efficiency of Experiment 3 was not as good as in Experiment 2 since more liquid solvent were trapped in the area where boiling occured. Hence, one may suggest that quick fracture heating (steam flooding type) rather than whole matrix heating (electrical heating type) or slow heating is more favorable to yield lower liquid solvent entrapment.

### 2.4.3 Effect of Solvent Type

The Thomson effect was proposed to explain the effect of pore size on the boiling temperature. The following equation describing this phenomenon indicates that lower temperatures are needed as the pore sizes get smaller to boil the liquid in porous media (Berg 2010).

$$T_r^S = T_\infty^S \exp(-\frac{2\sigma v^L}{r\lambda^{vap}}) \quad (1)$$

Where $\sigma$ is surface tension at the given temperature, $v^L$ is molar volume, $r$ is pore size radius, $\lambda^{vap}$ is heat of vaporization, $T_r^S$ is saturation temperature in the porous media, and $T_\infty^S$ is saturation temperature of the same liquid at the same pressure under bulk conditions.

One may also infer from Eq. 1 that the higher surface tension would lead to lower boiling temperature. For the heavier solvent, the boiling point temperature is higher and the energy required for bubble development is greater. At the same 70°C temperature, decane did not start to vaporize in the matrix as opposed to the heptane case (comparing **Fig. 2.8a** and Fig. 2.4d). After processing Fig. 2.8d and Fig. 2.8h, there were 6% and 13% of the matrix occupied by the trapped

liquid solvent. Unlike the heptane case, slow heating yielded lower amount of trapped liquid solvent in the matrix.

It was also observed that boiling was not very strong when temperature reached 100°C and using decane. Hence, due to longer heating time, decane in liquid phase gained more energy to vaporize and formed a stable network of bubbles. There was liquid solvent trapped by the bubbles but not as much as the heptane case in Fig. 2.6d. Owing to shorter heating time, vertical growth of vaporized solvent in Experiment 5 was less than in Experiment 4 as marked by the yellow line in Fig. 2.8d and Fig. 2.8h. The heat transfer and phase equilibrium critically affected solvent boiling. In Experiment 3, expanding/shrinking bubbles resulted in more solvent in liquid phase were trapped by bubbles (only considering the region where solvent was boiling) and small bubbles were isolated after losing connection with the network. Considering the above results, it is plausible to consider the heating rate and solvent type during the process design, in order to let the gas phase develop toward the throats and smaller pores so that they can be retrieved efficiently.

### 2.4.4 Effect of Wettability

The glass of the micromodel is naturally water-wet. To investigate the effect of wettability on the phase distribution, the wettability of micromodel was be altered by treating with SurfaSil liquid as suggested by Naderi and Babadagli (2011). When 20% or higher mass rate was applied, there was too much polymer coated the surface which risked plugging pores. After comparing the contact angle tests of series concentration, 15%-10% mass rate of Surfasil liquid was chosen for the experiments in this research. **Fig. 2.9** gives an idea of how the contact angle between oil and water was changed by this chemical. As Fig. 2.9b shows, the surface of the glass was efficiently altered to oil-wet.

Then, a series of experiments using oil-wet micromodel were designed (Experiments 7 and 8). After altering wettability, decane and heptane were injected in these experiments. Figs. 2.10a through 10f show the change of temperature at the testing points (on matrix and fracture of the micromodel). The red and blue curves represent fracture and matrix temperatures. The wetting behaviour of a certain liquid on the surface is related to surface potential, which may further affected the surface tension term. This, in turn, will change the temperature needed to boil the solvent.

The vaporization of solvent in oil-wet pores showed different patterns from the previous water-wet experiments. Bubbles appeared in fracture and matrix simultaneously, and the clusters of bubbles were dispersed in the micro-model as pointed out by red circles in **Fig. 2.11b**. With an increase in temperature, the gas bubbles in the matrix near the fracture expanded into the fracture to form a cluster as the yellow circle marked in Fig. 2.11g. The small bubbles existing in the fracture were gradually connected to each other and then merged into a larger bubble as shown in Fig. 2.10h and Fig. 2.10i. Also, the clusters of bubbles in the matrix were connected with each other to form a continuous network. The solvent in liquid phase were gradually drained by the expansion of the gas phase (compare the same location marked by yellow-squares in **Fig. 2.12**). Also, less liquid solvent was trapped by cluster of bubbles as the bubbles invaded the small pores and dead ends.

Close-up images of water-wet and oil-wet micromodels are shown in **Fig. 2.13**. In the water-wet model, solvent bubbles would not contact the walls of the pores (red circled part in Fig. 2.13a). More liquid solvent resided in narrow pores as well as dead end pores surrounded by by-passing bubbles. In the oil-wet micromodel, the bubbles expanded into small pores and throats and there

were no noticeable liquid solvent layers between the bubbles and the walls (red circled are in Fig. 2.13b). Less liquid solvent was trapped in the oil-wet model.

### 2.4.5 Effect of Oil Type and Viscosity

In Experiment 11, the process and model type (water-wet) were the same as Experiment 2 but heavier oil (600cp) was used in the matrix. Higher temperature was needed to start solvent boiling in Experiment 11. Therefore, one may observe that vaporization was slightly stronger in Experiment 2 than Experiment 11 when Fig. 2.6g and Fig. 2.14c (corresponding to the same temperature) are compared.

Experiments 12 and 13 were identical but more solvent was injected. In Experiment 12, a total 10ml heptane was introduced into the model and completely mixed with the mineral oil in the fracture and neighboring areas of the matrix after 12 hr (Fig. 2.14g). In Experiment 13, 16ml heptane was injected and a larger area in the matrix was occupied by oil/solvent mixture (compare Fig. 2.14g and 2.14m) and pure solvent. Likewise, more solvent in the liquid and gas form was drained out of matrix to the fracture in Experiment 13 at the same temperature level (compare Fig. 2.14h and 2.14n).

While heating, temperature at which the bubbles began to appear in Experiment 12 was slightly higher than in Experiment 13. In other words, the energy required for boiling was higher in Experiment 12. As less solvent injected in this experiment, smaller bubbles were formed (Fig. 2.14h) at a higher temperature. With less solvent bubbles existing in the pores, the expansion of oil/solvent mixture and drained amount to fracture was adversely affected. Despite higher temperature, the network of bubbles in the matrix and fracture feeding of gas and liquid solvents for Experiment 12 (Figs. 2.14j and 2.14k) are not as improved as in Experiment 13 (Figs. 2.14p and

k). In other words, a continuous network of solvent bubbles was obtained in Experiment 13 as seen in Fig. 2.14p.

Attention should also be given to the boiling temperature of the same solvent under different wettability conditions. In the oil-wet case, more bubbles appeared (Fig. 2.14p) compared to the water-wet equivalent case (Fig. 2.14c) of the same temperature indicating that lower temperatures are needed in the oil-wet case. This can be attributed to the interfacial tension existed in the pores. Eq. 1 implies that the change in the interfacial properties will result in a change in the boiling temperature and wettability alteration results in an alteration of interfacial tension. In Fig. 2.14q, the bubbles in the matrix (red circled part) would shrink and connect with the bubbles in the fracture and then a certain volume was observed to be produced. These observations were consistent with what we observed in the experiments using light oil.

### 2.4.6 Water Displacement Process

The hybrid solvent/thermal method is primarily based on expansion and "thermodynamic" recovery of oil and solvent rather than "displacement". Hence, after all these efforts that combine solvent and heating, water was injected to volumetrically replace oil/solvent through capillary imbibition (and gravity) in practice.

To displace the residual oil and solvent, water was injected at a rate of 1ml/hour after the systems has been cooled down to room temperature. The water gradually swept the pores and the distribution of fluids was recorded by camera. A series of snapshots are shown in **Fig. 2.15**. Water (in green color) filled the fracture (or wormhole) first and then started to imbibe into matrix (red circle in the first image).

Water-flooding performances of the oil- and water-wet cases are compared in **Fig. 2.16**. In both wettability conditions, the isolated gas bubbles (yellow circle in Fig. 2.16b) acted as an obstacle which diverted water toward the liquid filled pores indicated by yellow arrows. The IFT value between solvent and water was less than that of gas and water, and therefore, water invaded towards to the liquid phase. Meanwhile, gas bubbles became fragmented due to snap-off occurred at relatively small throats and then resulted in forming a cluster as illustrated by the changes in red square of Fig. 2.16a and Fig. 2.16b. Furthermore, the liquid solvent surrounding the bubbles was bypassed by invading water and remained. This can also be attributed to spreading phenomenon dictating that liquid solvent has more affinity to its vapor than to water. Due to favorable wettability, water displaced much more solvent/oil in Fig. 2.16h (water-wet) than in Fig. 2.16d (oil-wet).

**Figs. 2.17b** and **2.17c** illustrate the close-up images of the pores in oil-wet model experiments. The interface between oil and water showed neutral to oil-wet conditions. Also, besides the trapped oil/solvent in the dead end pores (red square in Fig. 2.17b), solvent/oil films were developed on the walls of the pores (yellow square in Fig. 2.17b). In the water-wet micromodels, residual solvent was in the form of filaments in the middle of the pores in Fig. 2.17a. The heavier oil version of water-flooding results is illustrated in Fig. 2.17c and more oil/solvent mixture was trapped by water.

## 2.5 Conclusions and Remarks

A micro-scale fluidic device was applied to visually study the solvent retrieval process in heterogeneous systems. After solvent injection to recover heavy-oil, the system was heated mimicking a thermal method to retrieve the solvent dissolved in the matrix oil

thermodynamically. The boiled solvent expanded out of the matrix also displacing the solvent (and oil mixed with it) in the liquid form towards the fracture. This process was evaluated for different wettability of matrix, oil viscosity, heating conditions ("point" heating from fracture or "plane" heating of the whole system), and heating rate.

The Kelvin effect and related equation was observed in all experiments indicating that temperature and energy requirement to vaporize the solvent was lower in porous media than in standard conditions. Heptane resulted in faster recovery of solvent under temperature effect than decane. From the calculation of the images, there was more liquid phase trapped by-passing bubbles in decane case than using heptane.

Oil viscosity did not affect the initiation of the vaporization of solvent but controlled the distribution of the bubbles. In heavier oils, the bubbles were more scattered and hard to form a continuous phase and a clustered network. The heating method (heating location and heating rate) controlled the bubble growth and solvent retention. Uniform heating showed that much more liquid solvent were trapped than fracture heating even the boiling was stronger. This indicates the importance of temperature gradient on the displacement of liquid and gas solvent. For the heptane case, the boiling was strong and less liquid solvent was trapped when applying higher heating rate. But in the decane case, the temperature requirement was much higher. Vaporization was not strong under the designed final temperature. Lower heating rate (slow heating) provided more chance to vaporize solvent in the smaller pores which eventually led to better retrieval. Therefore, one may suggest that quick fracture heating (steam flooding type) rather than whole matrix heating (electrical heating type) or slow heating is more favorable to yield lower liquid solvent entrapment in the lower carbon number solvent (heptane in our

experiments) case. Slow heating for the higher carbon number case (decane in our experiments) yielded lower amount of trapped liquid solvent in the matrix.

After the wettability was altered to more oil-wet, more isolated bubbles were observed than the water wet case. Marciales and Babadagli (2015) reported that bubbles preferred to grow into smaller pores and kept more stable in the oil-wet case. We also observed a similar behaviour and bubbles were recorded to be more scattered but eventually move to the fracture to be retrieved in the oil-wet case. In the water-wet cases, the bubbles grew into the matrix and were more connected to each other to form a continuous network. As the wetting behaviour affected the interfacial tension, the boiling temperature was observed to be reduced more in oil-wet experiments than water-wet experiments. This could be explained by the Thomson equation which implies that the interfacial tension affects the boiling temperature adversely. Through micro-model experiments, heating in oil-wet system showed a better performance of solvent retrieval.

The initial amount of solvent (or the composition of oil solvent mixture) before heating started, affected the final recovery of solvent. As more solvent existed initially, boiling started earlier and the bubbles were more continuous. While retrieving the solvent, the drive caused by solvent expansion in the vapor form helped further recovery of oil. Solvent boiling resulted in expansion of liquid oil/solvent mixture and resulted in a drive to push the liquid and vapor solvent out of matrix. But, this mechanism was unable to create sufficient drive force to retrieve enough amount of solvent to make the process practically viable. However, the oil in the matrix was conditioned through this process and it became less viscous. A final water-flooding was proposed to help displace the residual oil/solvent mixture in the matrix by taking advantage of reduced viscosity of oil through solvent dilution. After water-flooding, more liquid solvent were

trapped in oil-wet models. No significant change in the amount of solvent vapor entrapment was observed in oil and water-wet cases. The solvent vapor clusters were engulfed by the liquid solvent in the oil-wet case resulting in less efficient displacement by water in the oil-wet case.

## 2.6 References


Al-Bahlani, A.M. and Babadagli, T. 2008. Heavy-Oil Recovery in Naturally Fractured Reservoirs with Varying Wettability by Steam Solvent Co-Injection. Presented at the 2008 International Thermal Operations and Heavy Oil Symposium, Calgary, Alberta, Canada, 20-23 October. SPE-117626-MS. http://dx.doi.org/10.2118/117626-MS.

Al Bahlani, A.M. and Babadagli, T. 2009. Laboratory and Field Scale Analysis of Steam Over Solvent Injection in Fractured Reservoirs (SOS-FR) for Heavy Oil Recovery. Presented at the Annual Technical Conference and Exhibition, New Orleans, Louisiana, 4-7 October. SPE-124047-MS. http://dx.doi.org/10.2118/124047-MS.

Allen, J.C., Gillespie, R.E. and Burnett, D.B. Texaco Inc. 1984. Superheated Solvent Method for Recovering Viscous Petroleum. United States Patent 4.450.913.

Berg, J. 2010. *An introduction to Interfaces and Colloids, the Bridge to Nanoscience*. World Scientific Publishing Co. Pte. Ltd., Singapore.

Chang, J., Ivory, J.J., Forshner, K. and Feng, Y. 2013. Impact of Solvent Loss During Solvent Injection Processes. Presented at SPE Heavy Oil Conference-Canada, Calgary, Alberta, Canada. 11-13 June. SPE-165476-MS. http://dx.doi.org/10.2118/165476-MS.

Farouq Ali, S.M. and Abad, B. 1976. Bitumen Recovery from Oil Sands, Using Solvents in Conjunction with Steam. *J Can Petrol Technol* **15** (3): 80-90. PETSOC-76-03-11. http://dx.doi.org/10.2118/76-03-11.

Govind, P. A., Das, S. K., Srinivasan, S., and Wheeler, T. J., 2008. Expanding Solvent SAGD in Heavy Oil Reservoirs. Presented at International Thermal Operations and Heavy Oil Symposium, Calgary, Alberta, Canada, 20-23 October. SPE-117571-MS. http://dx.doi.org/10.2118/117571-MS.

Gupta, S., Gittins, S., Picherack, P. 2004. Insights into Some Key Issues with Solvent Aided Process. *J Can Petrol Technol*. **51** (2): 339-350. PETSOC-04-02-05. http://dx.doi.org/10.2118/04-02-05.

Nasr, T.N., Beaulieu, G., Golbeck, H. and Heck, G. 2003. Novel Expanding Solvent-SAGD Process "ES-SAGD". *J Can Petrol Technol* **42** (1): 13-16. PETSOC-03-01-TN. http://dx.doi.org/10.2118/03-01-TN.

Mohammed, M. and Babadagli, T. 2013. Efficiency of Solvent Retrieval during Steam-Over-Solvent Injection in Fractured Reservoirs (SOS-FR) method: Core Scale Experimentation. Presented at SPE Heavy Oil Conference, Calgary, Alberta, Canada. 11-13 June, Calgary, Alberta, Canada. SPE-165528-MS. http://dx.doi.org/10.2118/165528-MS.

Marciales, A. and Babadagli, T. 2016. Pore scale visual investigations on solvent retrieval during oil recovery at elevated temperatures: A Micromodel Study. Chemical Engineering Research and Design 106: 59-73.

Nasr, T.N., and Ayodele, O.R. 2005. Thermal Techniques for the Recovery of Heavy Oil and Bitumen. Presented at SPE International Improved Oil Recovery Conference in Asia Pacific, Kuala Lumpur, Malaysia, 5-6 December. SPE-97488-MS. http://dx.doi.org/10.2118/97488-MS.

Nasr, T.N. and Ayodele, O.R. 2006. New Hybrid Steam-Solvent Processes for the Recovery of Heavy Oil and Bitumen. Presented at SPE International Petroleum Exhibition and Conference, Abu Dhabi U.A.E, 5-8 November. SPE-101717-MS. http://dx.doi.org/10.2118/101717-MS.

Naderi, K. and Babadagli, T. 2011. Pore-scale investigation of immiscible displacement process in porous media under high-frequency sound waves. *J. Fluid Mech*. **680**: 336-360

Pathak, V. and Babadagli, T. 2010. Hot Solvent Injection for Heavy Oil/Bitumen Recovery: An Experimental Investigation. Presented at the Canadian Unconventional Resources and International Petroleum Conference, Calgary, Alberta, Canada, 19-21 October. SPE-137440-MS. http://dx.doi.org/10.2118/137440-MS.

Pathak, V., Babadagli, T. and Edmunds, N.R. 2011a. Mechanics of Heavy Oil and Bitumen Recovery by Hot Solvent Injection. Presented at the Western North America Regional Meeting, Anchorage, Alaska, 7-11 May. SPE-144546-MS. http://dx.doi.org/10.2118/144546-MS.

Redford, D. and McKay, A. 1980. Hydrocarbon-Steam Processes for Recovery of Bitumen from Oil Sands. Presented at the First Joint SPE/DOE Symposium on Enhanced Oil Recovery, Tulsa, Oklahoma, 20-23 April. SPE-8823-MS. http://dx.doi.org/10.2118/8823-MS.

Risk Reactor Inc.,www.riskreactor.com (accessed February 2014).

Shu, W.R. and Hartman, K.J. 1988. Effect of Solvent on Steam Recovery of the Heavy Oil. May, 1988: 457-564. SPE- 14223-PA. http://dx.doi.org/10.2118/14223-PA.

Zhao, L., Nasr, T.N., Huang, H. et al. 2004. Steam Alternating Solvent Process: Lab Test and Simulation. Presented at the Canadian International Petroleum Conference, Calgary, Alberta, 8-10 June. PETSOC-2004-044. http://dx.doi.org/10.2118/2004-044.

Zhao, L., Nasr, T.N., Huang, H. et. al. 2005. Steam Alternating Solvent Process: Lab Test and Simulation. *J Can Petrol Technol* **44** (9): 37-43. PETSOC-05-09-04. http://dx.doi.org/10.2118/05-09-04.

| Experiment No | Oil Type | Solvent Type | Heating Point | SurfSil Mass Rate | Wettability | Heating Rate |
|---|---|---|---|---|---|---|
| 1 | 250cp MO | heptane | fracture | 0 | water wet | slow |
| 2 | 250cp MO | heptane | fracture | 0 | water wet | quick |
| 3 | 250cp MO | heptane | fracture& matrix | 0 | water wet | quick |
| 4 | 250cp MO | decane | fracture | 0 | water wet | slow |
| 5 | 250cp MO | decane | fracture | 0 | water wet | quick |
| 6 | 250cp MO | decane | fracture& matrix | 0 | water wet | quick |
| 7 | 250cp MO | decane | fracture | 20% | oil wet | quick |
| 8 | 250cp MO | heptane | fracture | 15% | oil wet | quick |
| 9 | 250cp MO | heptane | fracture | 15% | oil wet | quick |
| 11 | 600cp MO | heptane | fracture | 0% | water wet | quick |
| 12 | 600cp MO | heptane | fracture | 15% | oil wet | quick |
| 13 | 600cp MO | heptane | fracture | 15% | oil wet | quick |

**Table 2.1—Oil type, solvent type and other parameters set for different experiments. MO: Mineral oil. SO: Silicon oil.**


Fig. 2. 1—Schematic of experiment set-up.

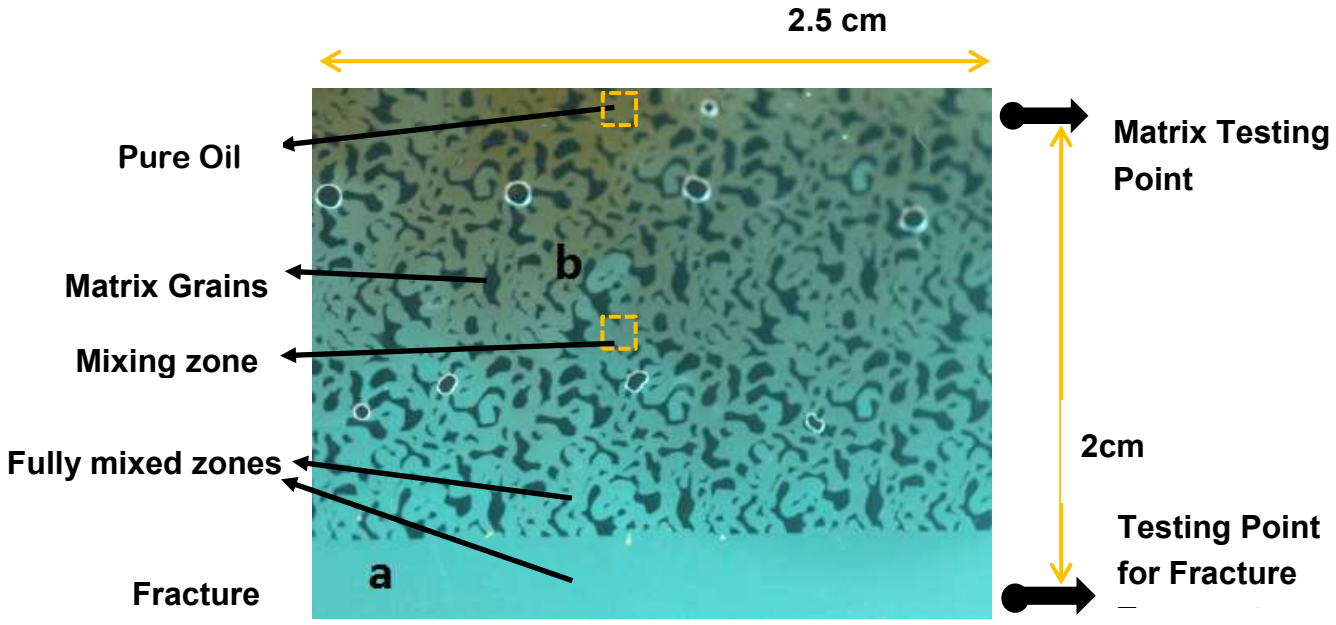


Fig. 2.2—Phase equilibrium after solvent injection: (a) solvent (in fracture); (b) solvent and mineral oil mixture.

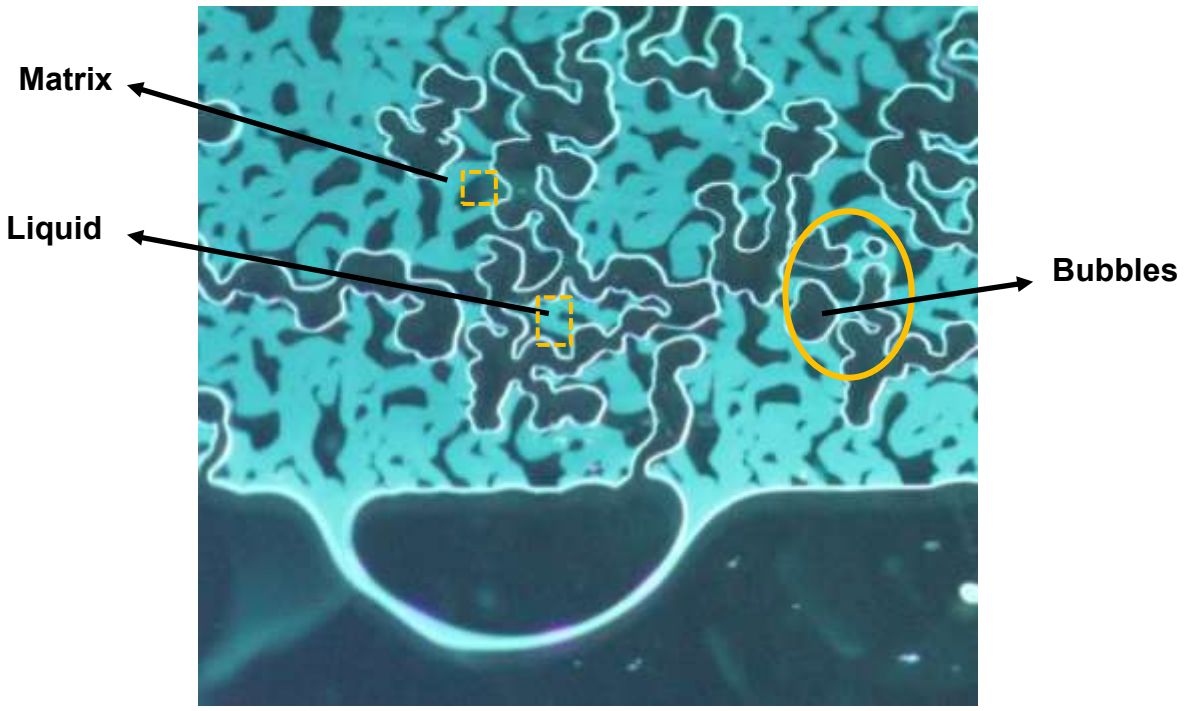


Fig. 2.3—Snapshot image during solvent (heptane) boiling.

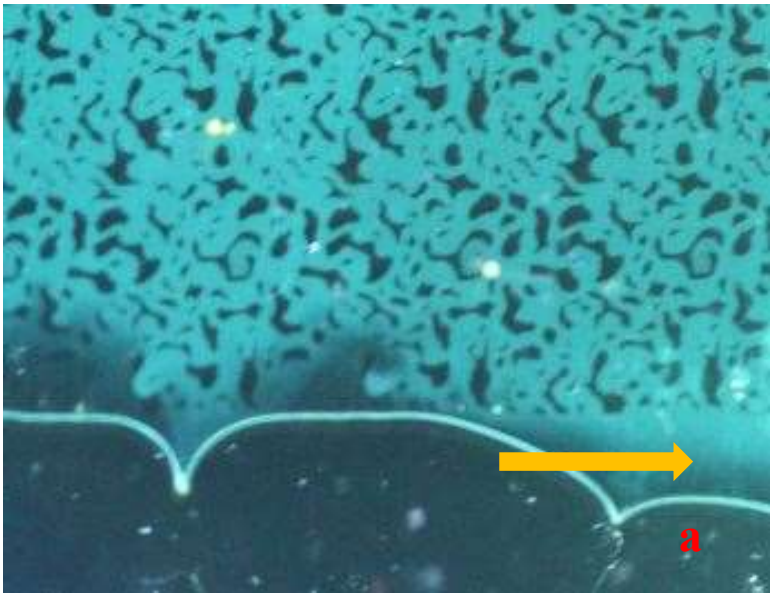

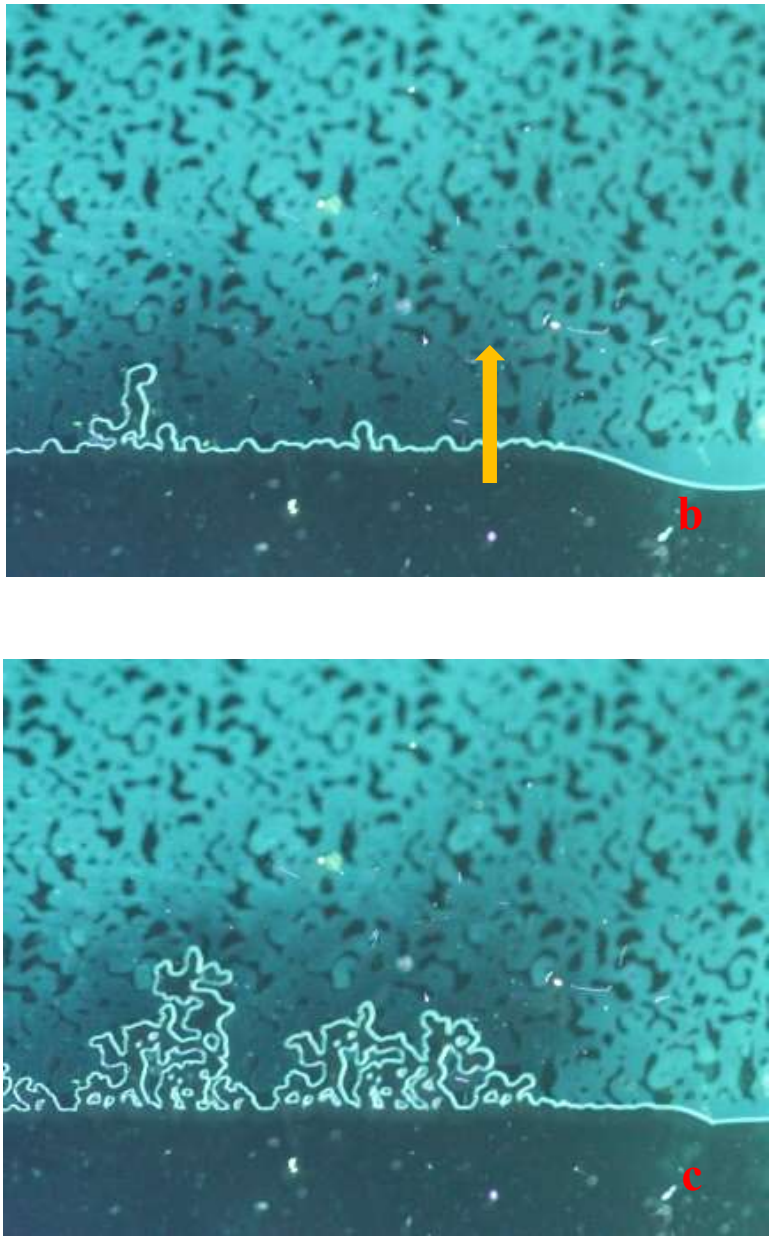


**Fig. 2.4—Development of solvent bubbles(heptane and water-wet case): (a) solvent firstly boiled in the fracture; (b) bubbles grew into the pores of the matrix connected with the fracture; (c) bubbles formed a cluster.**

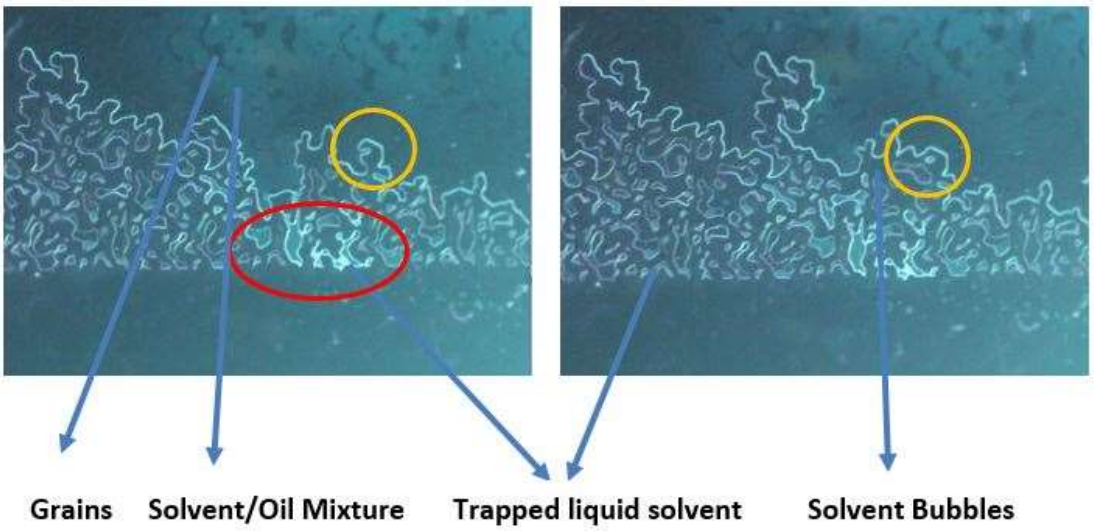


**Fig. 2.5—Microscopic views of solvent vaporization process (water-wet; heptane, and fracture-heating).**

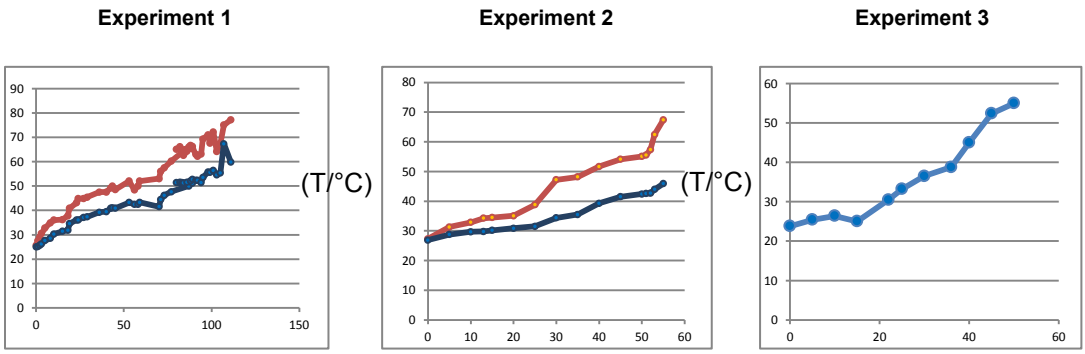


a) Heating Rate for Experiment 1 e) Heating Rate for Experiment 2 i) Heating Rate for Experiment 3

b) **55°C** in fracture, **42**°C matrix f) **55°C** in fracture, **42.4**°C matrix j) **45°C** in fracture and matrix

c) **60°C** in fracture, **47**°C matrix  g) **60°C** in fracture, **44**°C matrix  k) **50°C** in fracture and matrix

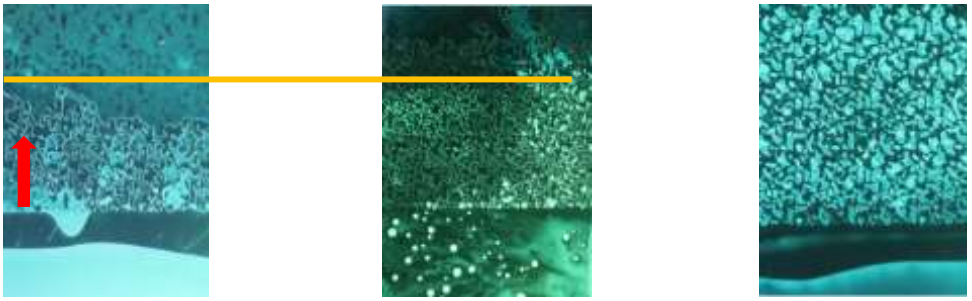

d) **70°C** in fracture, **54**°C matrix  h) **70°C** in fracture, **47**°C matrix  l) **55°C** in fracture and matrix

**Fig. 2.6—Pore-scale visualization of water-wet experiments injecting heptane (Experiment 1: slow heating; Experiment 2: quick heating; Experiment 3: whole micromodel heating).**

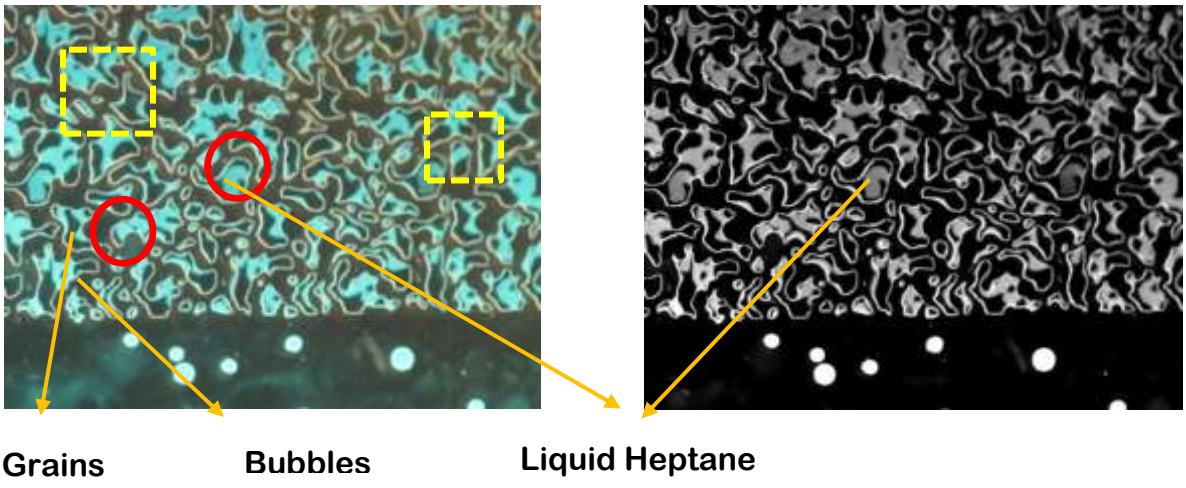


**Fig. 2.7—Close-up view of pores during uniform heating (saturation of gas phase in pores: 51.2%; saturation of liquid solvent: 48.8%).**

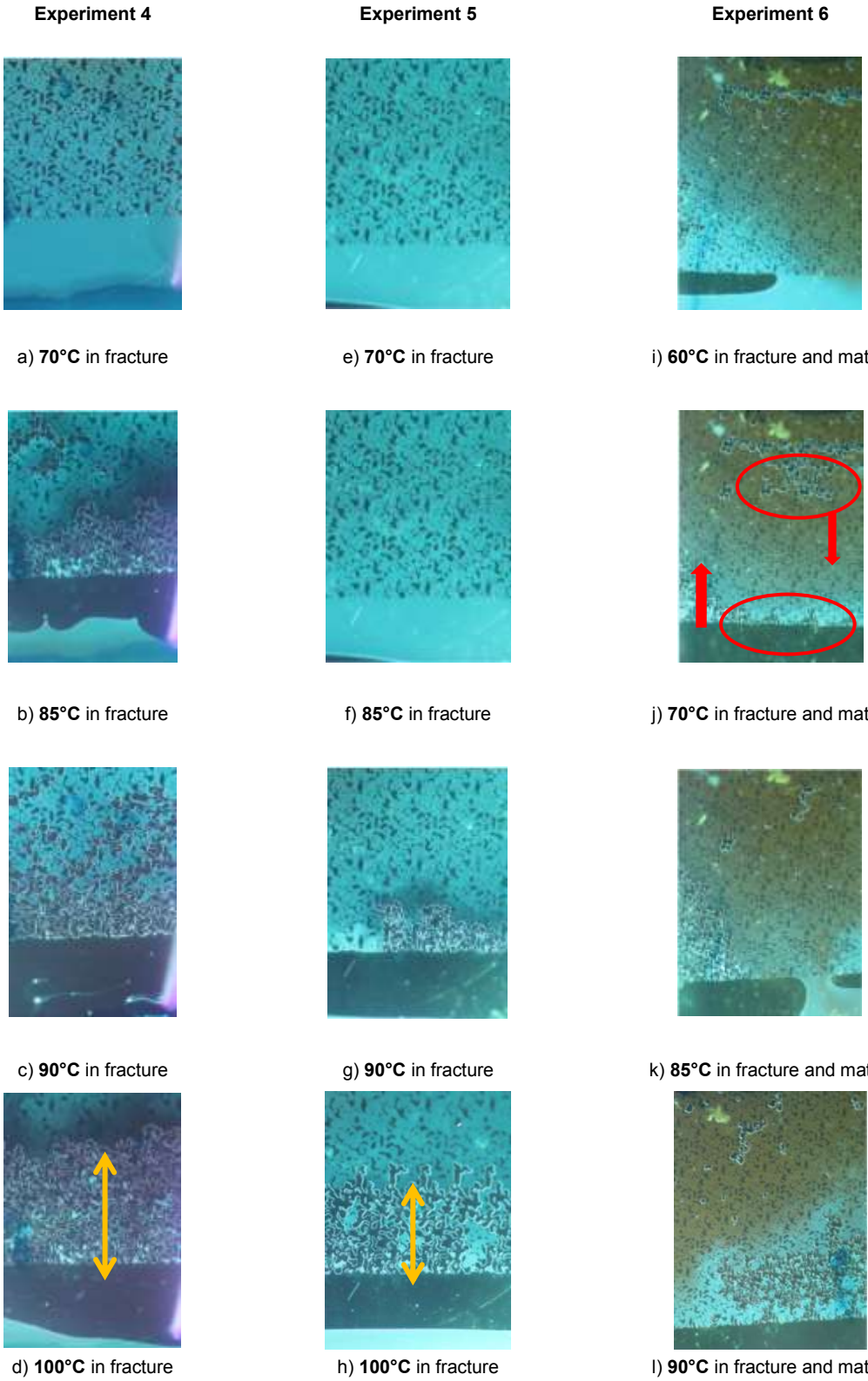


**Fig. 2.8—Pore-scale visualization of water-wet experiments injecting decane (Experiment 4: slow heating; Experiment 5: quick heating, and Experiment 6: whole micromodel heating).**

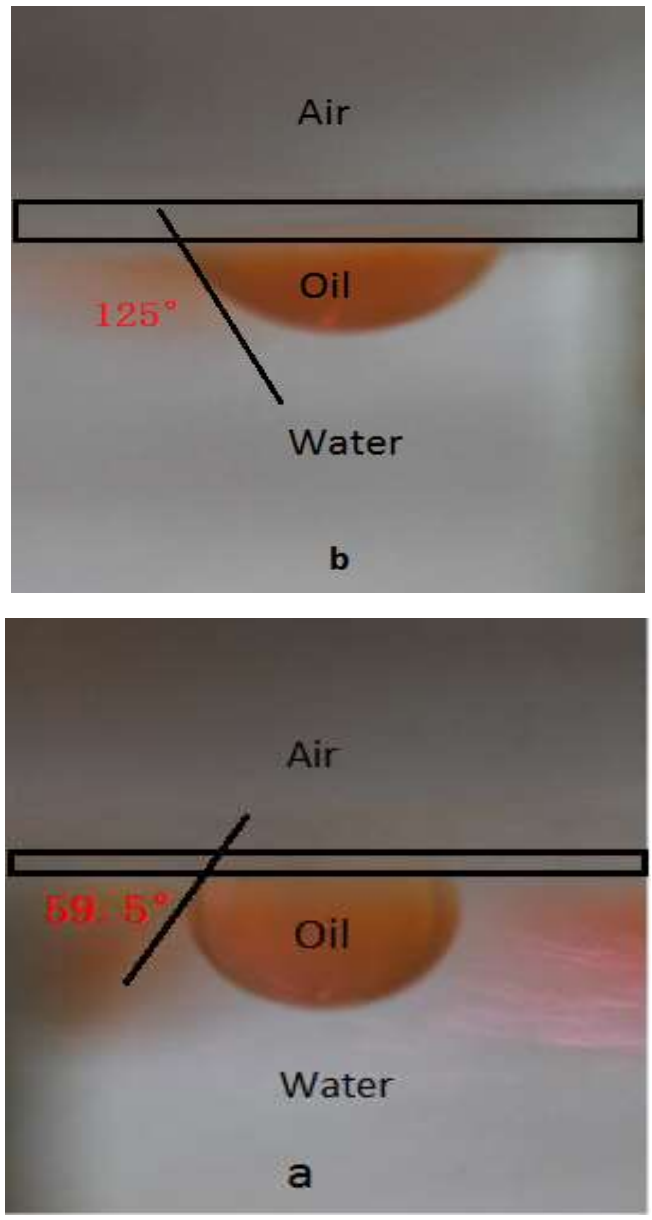


**Fig. 2.9—Contact angle test of glass surface between mineral oil and water before (a- water-wet) and after (b- oil-wet) treated by SurfaSil chemical.**

**Experiment 7**

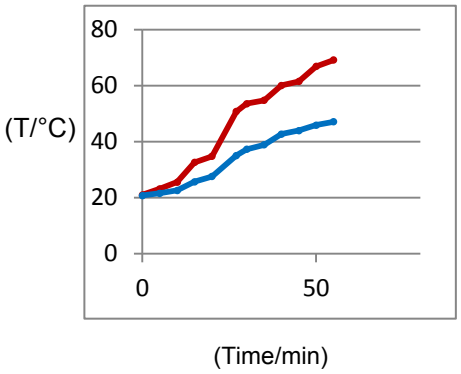


a) Heating Rate for Experiment 7

b) **51.3°C** in fracture, **36.1**°C matrix

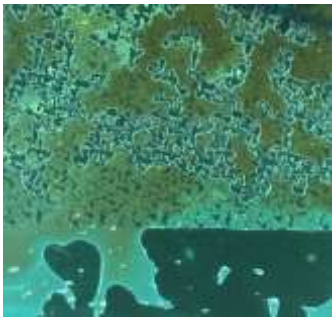

c) **53.6°C** in fracture, **37.3**°C matrix

**Experiment 8**

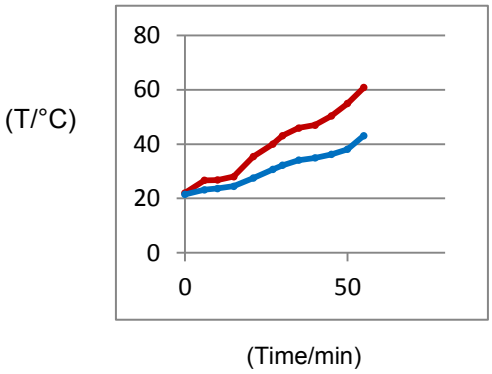


f) Heating Rate for Experiment 8

g) **47°C** in fracture and **33.7**°C matrix

h) **52.3°C** in fracture and **36.3**°C matrix

d) **59.9°C** in fracture, **42.5**°C matrix

i) **57.5°C** in fracture and **38.1**°C matrix

e) **69.2°C** in fracture, **47.1**°C matrix

j) **62.5°C** in fracture and **40.4**°C matrix

**Fig. 2.10—Visualization of solvent retrieval process when micromodel is oil wet (Experiment 7: decane & high heating rate; Experiment 8: heptane & high heaitng rate).**

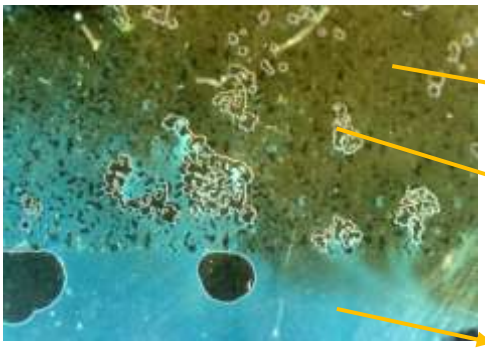


a) **45°C** in fracture and **33.7°C** in matrix

b) 2 minutes after Fig. a)

c) **50.3°C** in fracture and **36.3°C** in matrix

d) **60.5°C** in fracture and **40.4°C** in matrix

**Fig. 2.11—Visualization of solvent retrieval process of Experiment 9 when solvent is heptane and micromodel is oil-wet.**

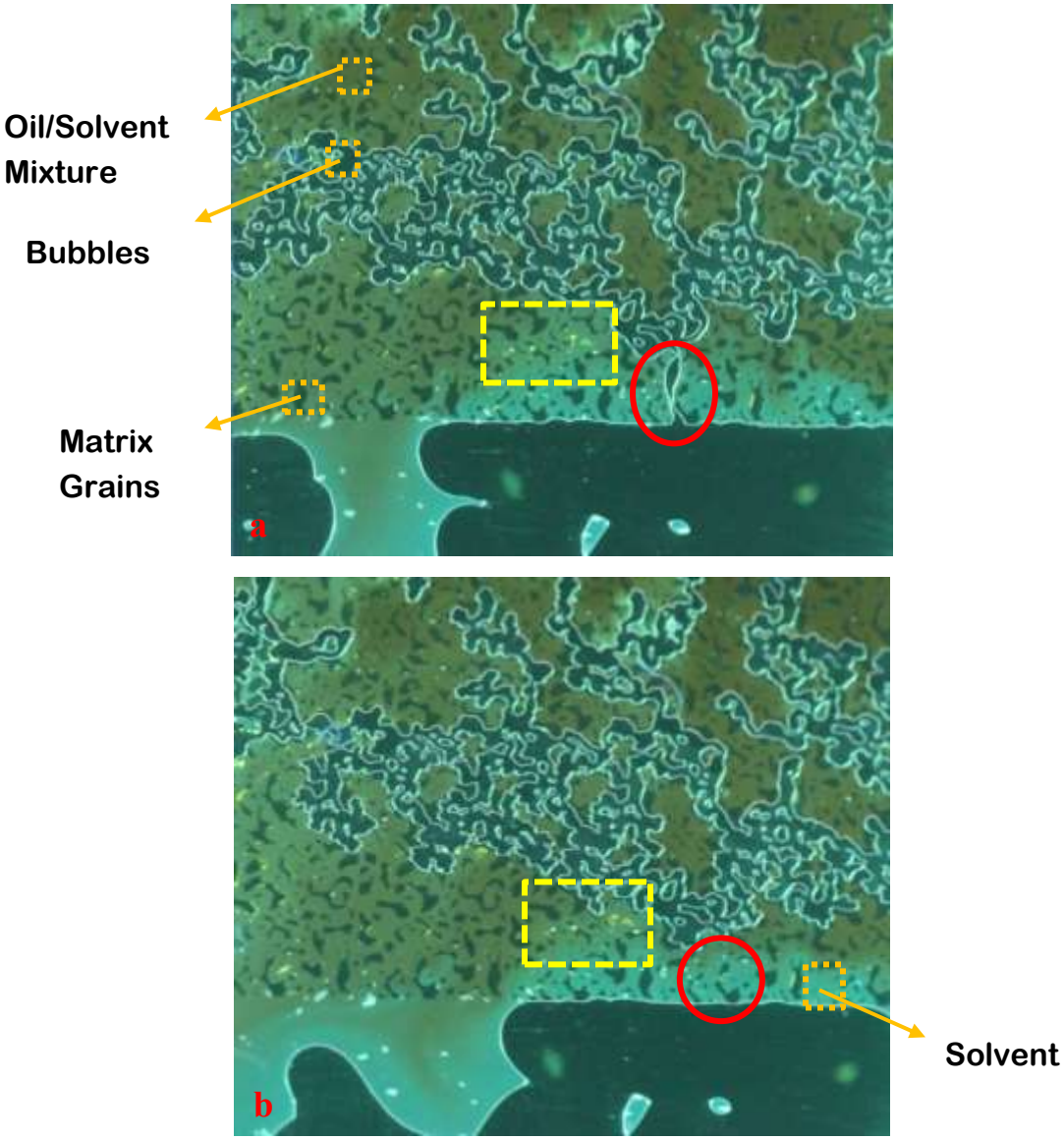


**Fig. 2.12—Snapshot images focusing on a certain point during Experiment 7 (decane; fracture heating).**

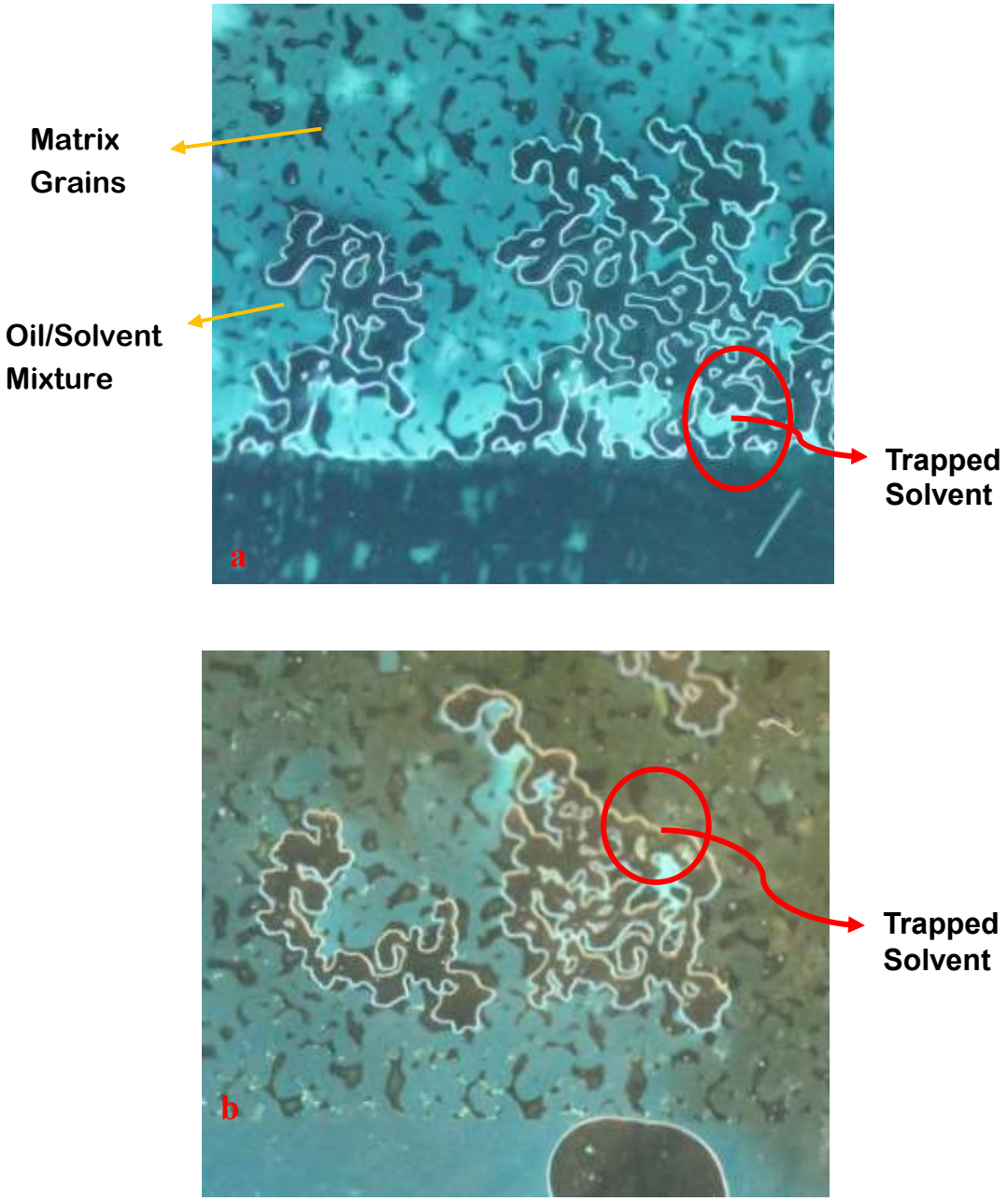


**Fig. 2.13—Close up images of gas phase distribution for both water-wet and oil-wet experiments: (a) water-wet and (b) oil-wet.**

**Experiment 11**

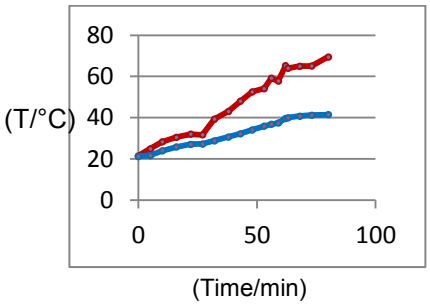


a) Heating Efficiency for Exp 11

b) **52.6°C** in fracture,**34.1°C** in matrix

c) **59.2°C** in fracture,**36.8°C** in matrix

d) **65.2°C** in fracture, **39.7°C** in matrix

e) **69.5°C** in fracture, **41.5°C** in matrix

**Experiment 12**

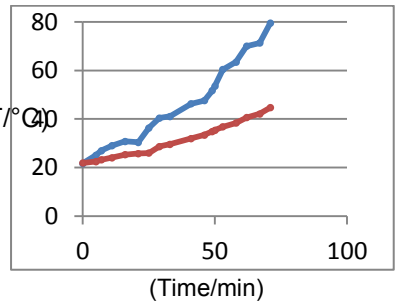


f) Heating Efficiency for Exp 12

g) **Initial Condition after solvent injection**

h) **53.6**°C in fracture, **35.4**°C in matrix

i) **60.4**°C in fracture, **36.8**°C in matrix

j) **69.2**°C in fracture, **47.1**°C in matrix

**Experiment 12**

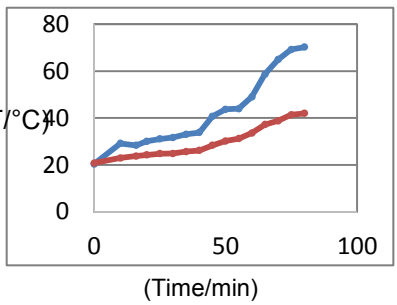


l) Heating Efficiency for Exp 13

m) **Initial condition after solvent injection**

n) **50.2**°C in fracture,**34.3**°C in matrix

o) **56.1**°C in fracture,**36.1**°C in matrix

p) **59.3**°C in fracture, **37.4**°C in matrix

k) **70**°C in fracture, **40.6**°C in matrix

q) **64.6**°C in fracture, **39.2**°C in matrix

r) **69.2**°C in fracture, **41.4**°C in matrix

**Fig. 2.14—Visualization of solvent retrieval process when using 600cp oil and heptane at 25°C( Experiment 11: water-wet, 16ml heptane injected; Experiment 12: oil-wet, 10ml heptane injected; Experiment 13: oil-wet and 16ml heptane injected).**

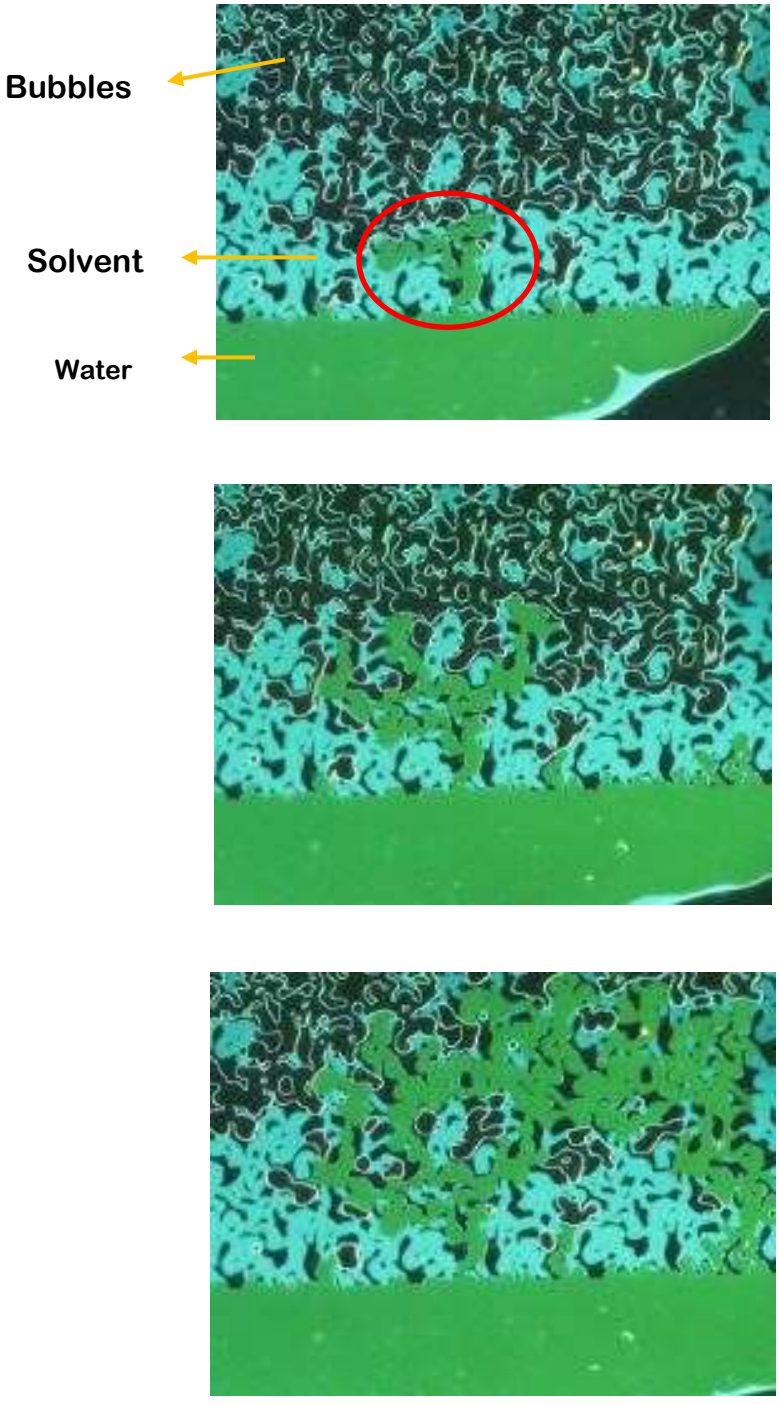


**Fig. 2.15—A series of images taken during the water itself gradually displaced the most of the bubbles.**

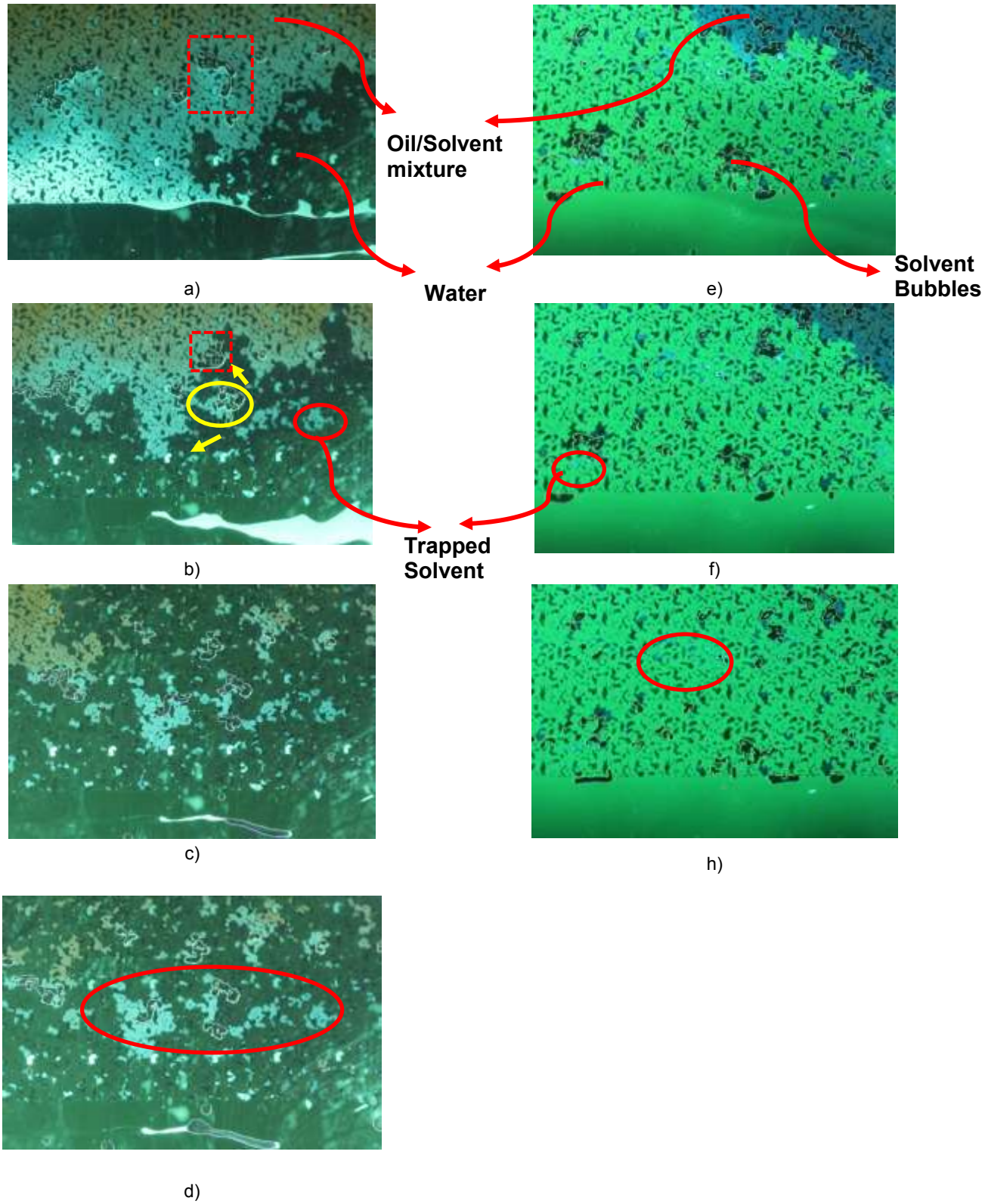


**Fig. 2.16—Water injection after solvent vaporization process: (a)—(d) oil-wet experiments using heptane and 200cp oil; (e)—(h) water-wet experiments using heptane and 200 cp oil.**

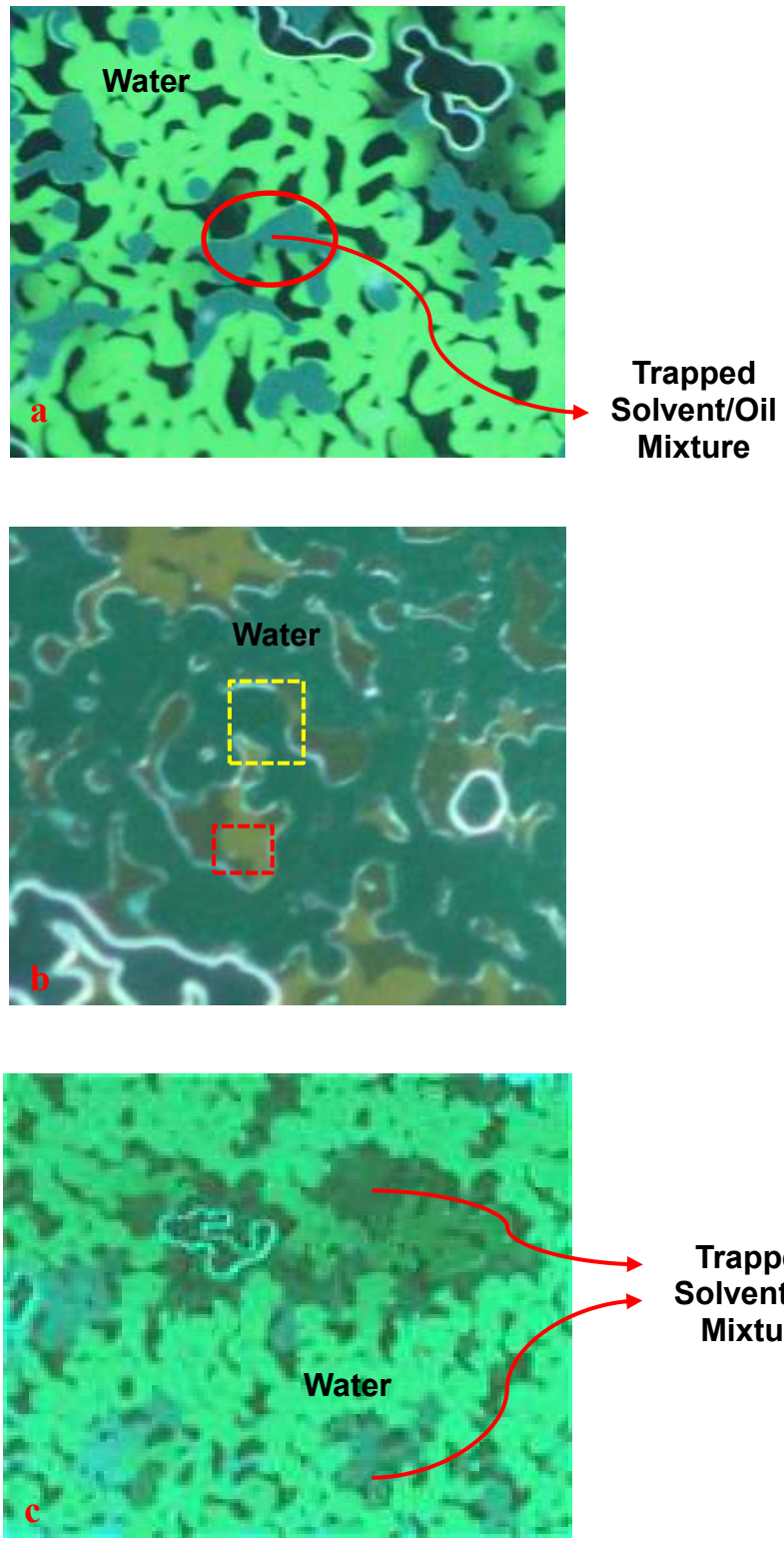


**Fig. 2.17—Close-up views of fluid distribution under different wettability conditions (a) water-wet condition and 200cp oil: Residual oil and solvent saturation= 14.97%; (b) oil-wet and 200cp oil: Residual oil and solvent saturation in pores = 26.23%; (c) oil-wet and 600cp oil).**

# CHAPTER 3: Use of New Generation Nano EOR Materials in Heavy-Oil Recovery by Chemical Flooding and Solvent Retrieval after Miscible Injection in Heterogeneous Reservoirs: Visual Analysis through Micro Model Experiments

A version of this chapter was presented and published at the SPE Annual Technical Conference and Exhibition held in Dubai, UAE, 26–28 September 2016 (SPE Paper 181320). It has also been submitted to a journal for publication.

## 3.1 Preface

Solvent injection has been given attention to enhance oil recovery by sole use or in combination with a thermal method to develop light and heavy-oil fields. To make this process efficient, one needs to retrieve the expensive solvent. In case of heterogeneous reservoirs (fractured carbonates or sands with wormholes), one needs to develop techniques other than viscous displacement to retrieve the solvent diffused into less permeable matrix portion. An alternative method other than previous thermal method is proposed to inject chemical solution to change the wettability and displace the matrix oil/solvent by capillary imbibition. Although it yields lower recoveries, injection of chemical solutions for the same purpose without pre-solvent treatment might be an efficient (more economical) EOR method.

A series of 2-D etched glass micromodel (sandstone replica with a fracture) experiments were designed to investigate the mechanics of chemical injection with and without pre-solvent injection. Conventional surfactants (sulfonate series) as well as new generation chemicals (nanofluids, ionic liquids) were tested for this purpose. After testing and screening effective chemicals without pre-solvent injection, the same chemicals were used to retrieve the solvent and recovery additional oil for pre-solvent injected systems. The micromodel was saturated by dyed processed oils and a selected solvent was injected through the fracture. After the solvent was diffused into matrix completely to recover the oil in it, the model was heated mimicking a thermal method to reach the boiling point of the solvent and retrieve it. Following the heating phase, aqueous phase was injected to retrieve the remaining solvent in the liquid or vapor phase.

## 3.2 Introduction

Heavy-oil recovery from heterogeneous systems is a challenge. In oil-wet carbonates or wormholed sands after CHOPS process, matrix oil recovery requires extra efforts involved in injecting expensive fluids. One option is to inject water containing chemicals that are capable of reducing interfacial tension (IFT) and alter wettability. This approach is cheaper but limited due to incapability of the injected fluid to reduce the viscosity of oil. Solvent is an option to achieve this if thermal methods are not practically applicable. In this case, one needs to retrieve the solvent during or at the end of the solvent treatment (Al-Bahlani and Babadagli 2011, 2012). This can be achieved by heating the medium to boil the solvent phase (Pathak et al. 2011, 2012, 2013). Depending on the solvent type, a great amount of solvent might be left after this treatment and one may need further waterflooding with wettability alteration chemicals to displace the liquid and vapor solvent and remaining matrix oil by capillary imbibition and gravity drainage (Mohammed and Babadagli 2013).

On the other hand, carbonate fractured reservoirs are mostly oil-wet, which indicates more complex recovery processes (Babadagli 2001, 2003). Surfactant as a valid tool to enhance oil recovery has been highly paid attention to apply in this type of reservoirs. Different kinds of surfactants depend on diverse functional mechanisms. During surfactant-based chemical flooding, wettability alteration or/and reduction of IFT were commonly confirmed to help achieve better access to the matrix and higher sweep efficiency (Babadagli 2003; Seethepalli et al. 2004; Lohne and Fjelde 2012; Stukan and Abdallah 2012).

In heavy oil systems, high viscosity limits the effect of reducing interfacial tension. In this case, chemicals which could generate low viscosity emulsions can be practically applied (Okandan

1977; Liu et al. 2006; Bryan and Kantzas 2009). Surfactants have been proposed to produce the mixture of solvent and heavy oil in the form of liquid and vapor after the solvent/thermal methods (Mohammad and Babadagli 2013, 2016). Mohammed and Babadagli (2016) reported contact angle and imbibition test results indicating the capability of chemical injection to retrieve the expensive solvent by wettability alteration in fractured sands and carbonates. This type of core scale experiments revealed useful information and promising chemicals; yet, pore-scale work is needed to better understand this process and gain more data to design optimal application conditions for such expensive EOR methods.

Chemical types are abundant for this kind of application. Commonly microemulsion phase behavior and IFT tests are applied to screen chemicals. Barnes et al. (2010) designed a series of micro-emulsion tests to visualize the volume and quality of the microemulsion phase to estimate their efficiency. The tests (contact angle tests and AFM tests), which could indicate the wetting behaviour of surface, were widely used to investigate the chemicals (Kumar et al. 2008; Stukan and Abdallah 2012).

Micro-fluidic devices are suggested as a tool to simulate the displacement process under reservoir conditions. Jamaloei et al. (2009) investigated the dilute surfactant flooding in both oil-wet and water-wet micromodels to discuss the effect of wettability. Hematpour et al. (2012) utilized the micromodel to estimate the role of concentration in surfactant-flooding process. Howe et al. (2015) observed the existence and displacement microemulsion process in micromodels.

In the present study, the behavior of different chemicals was investigated while they were injected to displace heavy-oil (first group of experiments, chemical flooding onl) or heavy-oil

solvent mixtures (second group of experiments, chemical injection after solvent injection and heating for solven retrieval) through visual pore scale displacement experiments. The mechanics of matrix-fracture interaction to retrieve solvent and recover heavy oil was visually analyzed. More practical information is provided by suggesting successful chemicals and their optimal use.

## 3.3 Experimental Methodology and Procedure

### 3.3.1 2-Dimensional Visualization System

The 2-D visualization system includes a Berea-sandstone-replica heterogeneous glass model, syringe pump, UV light, associated tubes/connections, and camera. The etched glass model was made according to the procedure suggested by Naderi and Babadagli (2011). There was a conduit etched nearby the matrix part to represent the fracture or wormhole. Two ports were drilled at the two ends of the fracture/wormhole side to introduce and discharge the fluids into the system. A syringe pump was used to keep the injection rate constant at 0.06ml/hr. A fixed visual window (marked by a square in **Fig. 3.1**) was set on the middle part of the micromodel to observe the displacement process in simulated fractured/worm-holed system avoiding the edge effects.

### 3.3.2 Chemicals and Properties

Mineral oil (MO) and heptane were chosen as the oil and solvent phases and their properties are listed in **Table 3.1**. Six chemicals were selected based on previous experiences for the chemical flooding experiments. All chemical flooding tests were conducted at ambient conditions (room temperature, 22°C). **Table 3.2** displays the properties of the chemicals. Wei and Babadagli (2016) tested the IFT of nano-fluids with heavy oil under variable temperatures. Referring to their data, the IFT values of selected surfactants in certain concentration (with heavy oil 6000cp at 25°C)

are listed in **Table 3.3**. Proper dying agents were selected to help distinguish different phases: DFSB-K175 for MO, DFSB-K43 for heptane and IFWB-C8 for chemical solution from Risk Reactor (2014). Under UV light, MO, grains, solvent and aqueous phase are shown as brown, black, cyan and green in the experiments, respectively, throughout the experiments.

In order to investigate the mechanism and evaluate the surfactants, a series of glass-tube tests and microfluidic experiments were implemented. The microemulsion development and stability tests were firstly performed for the sulfonate series surfactants. Then all chemicals were injected into the micromodels to visualize their displacement and wettability alteration/IFT reduction capacities. A comparative analysis of the performances was done by focusing only on one area in the models for all cases. The detailed parameters of experiments are given in **Table 3.4**.

## 3.4 Results and Discussion

### 3.4.1 Glass-Tube Experiments

Microemulsion -tube- tests reveal valuable information about the efficiency and stability of surfactants. The presence of undesirable phases (macro-emulsion or gels) and time required to equilibrate are observed before using the surfactants in practice (Barnes et al. 2008). These tests were set using the same parameters: surfactant at 1%wt in the aqueous phase using de-ionized water, room temperature, same mineral oil (1:1 volume ratio) and without co-solvent.

The mixtures of oil and solution were made in different tubes and their volumes were measured and recorded and, as in **Fig. 3.2a**, flat oil-water interfaces were observed. Then, these cap-tubes were shaken manually to provide enough shear force to emulsify and then changes of the interface were observed at certain intervals of time. The low interfacial tension helped form smaller oil droplets surrounded by the surfactant. The formation of different types in the

mixtures and the time to stabilize reflected the potential of these chemicals. On the other hand, these results worked with the following microfluidic experiments to screen these surfactants. It was illustrated that large oil globules (gel phase) existed in Tube A and Tube C marked by the black square in Fig. 3.2c, the size of oil globules was larger in Tube C than in Tube A. In Tube B, the micro-emulsion phase was stable and gentle. From micro-emulsion stability point of view, Surfactant B was seen to be the most efficient among this series.

### 3.4.2 Microfluidic Experiments

After the micromodel was saturated with the same MO, dyed water was firstly injected from one port to simulate initial water flooding. In the first two experiments, the wettability of the micromodel was initially water-wet or neutral-wet. There was only a small amount of water imbibing into the matrix part after 20 h of continuous injection. It is illustrated that most of the injected water preferred the path through fracture and left large amount of un-swept oil in matrix. Then 1%wt chemical solution was added to the flooding system and immediately flooding front started to invade into the pores of the matrix. The first 7 h of injection in three experiments was recorded and compared in **Fig. 3.3c**. It is interesting that these surfactants of the same series showed a different behaviour consistent with the glass-tube tests.

In Experiment 1, the flooding front was stable and almost uniform at early stage, which showed promising behaviour as can be inferred from Fig. 3.3b. But, after nearly two hours of injection, it is obvious that a flow of oil was drained into the fracture and then the communication between matrix and fracture was established (at least in the portion of the observation window). The oil existed in the form of small blobs (emulsion but different size droplets) and part of them had been drained back and produced through fracture during following displacement process.

The counter-current flow was maintained between the fracture and matrix part. But bank of oil blobs (marked in yellow circle in **Fig. 3.4**) still existed in the pores near the fracture after long-term displacement, which reduced the recovery factor. In Fig. 3.4, the area used as observation window was totally swept. In the pores distant from the fracture, the displacement process was efficient and residual oil existed in form of small blobs as marked by a square in Fig. 3.4. Smaller oil blobs were carried by the chemical solution to the fracture and then to the production port meaning that the droplets much smaller than pores flow as a pseudo single-phase fluid (Dennis 2008). Also, some small oil droplets attached to the walls of surface and thus were hard to mobilize. Larger oil blobs (pointed out by a red square) were trapped, which required more force or shear rate to overcome the capillary force.

Surfactant B (Experiment 2) showed a similar performance. A displacement front was formed once the chemical solution started to imbibe into the matrix as illustrated in Fig. 3.3j. But there was no obvious flow of MO as in the previous experiment. The water front initially grew not as quickly as in Experiment 1 but more stably and neatly, which led to a better displacement/recovery. The oil droplets of different scales were spread and trapped in the pores. Mostly, the oil was trapped in dead ends and small throats where there was no enough force to resist the capillary force as indicated by red squares in **Fig. 3.5**.

As different from the other two experiments, the wettability of the micromodel in Experiment 3 appeared to be more water-wet and water injected started to imbibe into the matrix after a while. As illustrated in Fig. 3.3q, the initial 20-hour water displacement resulted in rough water front and obvious trapped oil indicating a degree of water wetness but not very strong. Fig. 3.6 provides two images for water and chemical flooding to be compared. The residual oil was in the form of slugs and small fragments plugging throats with no sign of mobility (Fig. 3.6a); then,

surfactant flooding started. The addition of surfactant resulted in reducing interfacial tension between oil and aqueous phases and further causing emulsion. The trapped oil at the interface between matrix and fracture was mobilized and produced through fracture. Increasing mobility (marked by red square) assisted on gradually enhancing sweep efficiency. Meanwhile, the surfactant solution allowed the oil droplets to coalesce (indicated by red circles in Fig. 3.6a and 3.6b).

After the microscale analysis of the behaviour of the surfactant flooding, the images from the fixed observation area were processed to calculate the recovery factor before and after chemical injection. The results are given in **Fig. 3.7**. The flow of oil blobs back to the matrix reduced the invasion efficiency and further limited the recovery factor by Surfactant A. But the phenomena also provided a chance that further displacement was effective. These micromodel experiments provided a good tool to understand the micro-scale mechanism and screen efficient surfactant. In agreement with the tube tests, the Surfactant B achieved the best result among these series and was chosen as the surfactant to be used in the pre-solvent injection cases.

Besides these sulfonate surfactants, ionic liquid and nanoparticle solutions were also applied in chemical flooding experiments following the same procedure (**Fig. 3.8**). These chemicals were efficient wettability altering agents (Mohammed and Babadagli 2016). It was also observed that nano-fluids might affect more on fluid/rock interactions than fluid/fluid interactions. With the same injection rate, the aqueous phase gradually swept the pores in matrix with less oil trapped than water injection. The displacement front was rougher and moved faster initially unlike the surfactant cases. But, it is noticeable that in the fracture part, small oil droplets were spread as shown in yellow circles in Figs. 3.8c and 8d after the initial stage of injection and water front reached its limited depth into the matrix system.

**Fig. 3.9** shows oil trapping mechanics after surfactant flooding. The interface between the MO and aqueous phase was not changed noticeably as opposed to the three surfactant experiments. The length of oil patches was longer than the previous surfactant experiments (marked by a square in Fig. 3.8). When using $Al_2O_3$, the fingering phenomena was even more obvious and left more and longer bypassed oil blobs. The front of aqueous phase near the edge of the matrix (the red circled part in **Fig. 3.10**) moved faster and broke through more obviously. In the pores marked by the square in Fig. 3.10, the aqueous phase existed in the form of filaments and there was noticeable thin layer between the two phases.

Comparing these three nano-fluids, it is obvious that they did not affect the fluid-fluid properties critically. One may conclude with this observation that their main functional role is wettability alteration compared to changing the interfacial properties between the oil and aqueous phases (compare the images in Figs. 3.9 and 10 with the one in Fig. 3.6a). As for the residual oil saturation, ionic liquid was asserted to be the most efficient among these three unconventional EOR chemicals.

### 3.4.3 Solvent Retrieval Experiments

In the second group of experiments, chemical flooding was applied after solvent injection (and then heating) experiments to test the capability of chemicals in retrieving the remaining solvent in the matrix (in the form of vapor and/or liquid). The most efficient surfactant (Surfactant B was observed to be the one which yielded the strongest matrix transfer as seen Fig. 3.3) was injected at rate of 1ml/hr to the model after solvent injection (**Fig. 3.11**). In this case, a large amount of liquid heptane mixed with mineral oil in the pores of the matrix existed with pure mineral oil. When the aqueous phase invaded into the matrix, the solvent was drained into the pores further

with obvious fingering phenomena even certain amount of fluids in the pores were produced through the fracture. After a successful trial of chemical injection (strong matrix invasion by chemical solution) preceded by solvent treatment, another group of chemical injection experiments were performed. In these trials, the solvent first retrieved by heating (thermal application as done in the first round of experiments) and a final round of water-flooding with chemical additives was carried out to displace more solvent/heavy-oil form the matrix by wettability and interfacial tension alteration.

After saturating the micromodel with MO, heptane was injected until it totally mixed with the oil. Then, the model was heated to the boiling point of the solvent to mimic a thermal method. Through this process, the solvent was converted into vapor phase and became more mobile to flow to the fracture/wormhole part to be retrieved. However, a great amount of solvent was still remained in the form of liquid and vapor entailing an application of water injection. Fig. 3.12 shows images until this stage (the boiling of solvent and the development and nucleation of bubbles).

Under the oil-wet conditions, the bubbles appeared to be trapped in the pores of the matrix and then gradually expanded and connected with each other to form a cluster (Cui and Babadagli 2016). Vapor solvent expanded into the fracture and was produced through the production port. Along with the production of gas bubbles, the liquid solvent and some MO was also carried toward the fracture during this process. This simulated process reflected the pore-scale mechanism of solvent retrieval and related process was discussed in another paper (Cui and Babadagli 2016).

After this process (solvent retrieval by heating), 1wt% ionic liquid was injected (after cooling the sample to the room temperature) to displace the residual solvent and oil in the matrix by capillary imbibition altering the wettability. The images taken during this process is shown in **Fig. 3.13**. The residual solvent bubbles changed their shape and their connection was broken. The smaller bubbles developed this way started to invade the aqueous phase. The small and isolated bubbles (pointed out by red circle in Fig. 3.13d) finally were trapped in pores, and the sweep efficiency of ionic liquid was confirmed to be promising.

After the heating procedure to retrieve solvent and recover additional heavy-oil, a chemical (SiO2) solution was injected to displace all the residual phases (solvent and heavy-oil). Due to the wettability alteration and IFT reduction caused by this nano-fluid, the aqueous phase imbibed into the pores overcoming the capillary force and efficiently drained the residual pore-fluids. Some of the isolated bubbles in the porous media were mobilized into the fracture as a result of matrix-fracture -imbibition- interaction. As similar to the previous displacement results, long patches of oil were trapped near the interface between the matrix and fracture (marked by red circles in **Fig. 3.14c**).

Finally, Surfactant B was tested as it was the most effiicient one among the sulfonate series surfactants in the previous runs. It was injected into the system to recover the residual phases of the heavy-oil and solvent following the same procedure. The imbibition grew faster with higher sweep efficiency with it (**Fig. 3.15d**). There existed trapped oil around the gas bubbles (red circled in Fig. 3.15d) and in the dead ends as being different from the previous case with SiO2 (longer patches of oil trapped as seen in Fig. 3.14). Surfactant B showed the most promising result with least oil and solvent trapped under the observed area.

## 3.5 Conclusions

Mircofluidic devices provided a tool to simulate the small scale heterogeneity and reflect its role in displacement of heavy-oil by chemical flooding. Chemical screening was achieved for heterogeneous systems (fractured or worm-holed) and micro-scale mechanism of wettability alteration and interfacial tension change (micro-emulsion development) was analyzed visually.

Surfactants reduced the IFT between the oil and aqueous phase, which mobilized some trapped oil in pores of the matrix part near the fracture. A bank of small oil blobs existed due to crossflow between matrix and fracture when using Surfactant A. When front moved on toward the matrix (far from the fracture), no similar structure of oil bank was observed.

Among the three surfactants used, Surfactant B resulted in not only a faster movement but also a stable-front displacement. Also, very small-size oil blobs were mobilized and carried by the aqueous phase even when the front moved further away.

Nanofluids showed a different behaviour than surfactants. There was limited interaction between the oil and aqueous phase in the form of noticeable thin layers of particles. An interface development between the grains and fluids were more noticeable and this caused improved capillary imbibition (by wettability alteration) to displace more oil and solvent.

After selecting more efficient chemicals, the solvent retrieval process was simulated and visualized in the 2-D micromodels. After comparation of final oil recovery and solvent retrieval, Surfactant B achieved best result among the selected chemicals under experimental conditions. The imbibiton of aqueous phase was faster and neat when using surfactant B compared to the cases with SiO2 and ionic liquid. The saturation of residual oil and solvent was much lower with ionic liquid and Surfactant B compared to SiO2.

When solvent was pre-injected into the system, it helped dilute the heavy oil and made the frontal movement of succeedded aqueous phase (with chemicals) imbibition into the matrix.

## 3.6 References


Abdallah, W. and Stukan, M. 2012. Interfacial Tension (IFT) and Surface Alteration Interplay. Presented at Abu Dhabi International Petroleum Conference and Exhibition, Abu Dhabi, UAE, 11–14 November . SPE-161279-MS. http://dx.doi.org/10.2118/161279-MS.

Al-Bahlani, A.M. and Babadagli, T. 2011. SOS-FR (Solvent-Over-Steam Injection in Fractured Reservoir) Technique as a New Approach for Heavy-Oil and Bitumen Recovery: An Overview of the Method, *Energy and Fuels* **25**: 4528–4539.

Al-Bahlani, A.M. and Babadagli, T. 2012. Laboratory Scale Experimental Analysis of Steam-Over-Solvent Injection in Fractured Reservoirs (SOS-FR) for Heavy-Oil Recovery. *J. Petr. Sci. and Eng.* **84-85**: 42-56.

Babadagli, T. 2001. Scaling of Co-Current and Counter-Current Capillary Imbibition for Surfactant and Polymer Injection in Naturally Fractured Reservoirs, *SPE Journal* **465–478**.

Babadagli, T. 2003. Evaluation of EOR Methods for Heavy-Oil Recovery in Naturally Fractured Reservoirs, *J. of Petroleum Science and Eng.* **37** (1-2): 25–37.

Barnes, J. R., Smit, J., Smit, J. et al. 2008. Development of Surfactants for Chemical Flooding at Difficult Reservoir Conditions. Presented at SPE Symposium on Improved Oil Recovery, Tulsa, Oklahoma, USA, 20–23 April. SPE-113313-MS. http://dx.doi.org/10.2118/113313-MS.

Barnes, J. R., Smit, J., Smit, J. et al. 2008. Development of Surfactants for Chemical Flooding at Difficult Reservoir Conditions. Presented at SPE Symposium on Improved Oil Recovery, Tulsa, Oklahoma, USA, 20–23 April. SPE-113313-MS. http://dx.doi.org/10.2118/113313-MS.

Bryan, J. and Kantzas, A. 2009. Potential for Alkali-Surfactant Flooding in Heavy Oil Reservoirs Through Oil-in-Water Emulsification. *J Can Petrol Technol*. **48** (2): 37–46. PETSOC-09-02-37. http://dx.doi.org/10.2118/09-02-37.

Denney, D. 2008. Enhanced Heavy-Oil Recovery by Alkali/Surfactant Flooding. *JPT* **60** (03): 91–93. SPE-0308-0091-JPT. http://dx.doi.org/10.2118/0308-0091-JPT.

Hematpour, H., Arabjamloei, R., Nematzadeh, M. et al. 2012. An Experimental Investigation of Surfactant Flooding Efficiency in Low Viscosity Oil Using a Glass Micromodel. *Energy Resources.* **34** (19): 1745–1758. http://dx.doi.org/10.1080/15567036.2010.490821.

Howe, A.M., Clarke, A., Mitchell, J. et al. 2015. Visualizing Surfactant EOR in Core Plugs and Micromodels. Presented at the SPE Asia Pacific Enhanced Oil Recovery Conference. Kuala Lumpur, Malaysia, 11–13 August. SPE-174643-MS. http://dx.doi.org/10.2118/174643-MS.

Jamaloei, B. Y., Kharrat, R., and Ahmadloo, F. 2009. Selection of Proper Criteria in Flow Behavior Characterization of Low Tension Polymer Flooding in Heavy Oil Reservoirs.

Presented at Kuwait International Petroleum Conference and Exhibition, Kuwait City, Kuwait, 14–16 December. SPE-127606-MS. http://dx.doi.org/10.2118/127606-MS.

Kumar, K., Dao, E.K., and Mohanty, K.K. 2008. Atomic Force Microscopy Study of Wettability Alteration by Surfactants. *SPE J.* **13** (02): 137–145. SPE-93009-PA. http://dx.doi.org/10.2118/93009-PA.

Liu, Q., Dong, M., and Ma, S. 2006. Alkaline/Surf actant Flood Potential in Western Canadian Heavy Oil Reservoirs. Presented at SPE/DOE Symposium on Improved Oil Recovery, Tulsa, Oklahoma, USA, 22–26 April. SPE-99791-MS. http://dx.doi.org/10.2118/99791-MS.

Lohne, A. and Fjelde, I. 2012. Surfactant Flooding in Heterogeneous Formations. Presented at SPE Improved Oil Recovery Symposium, Tulsa, Oklahoma, USA, 14–18 April. SPE-154178-MS. http://dx.doi.org/10.2118/154178-MS.

Mohammed, M. A., and Babadagli, T. 2016. Experimental Investigation of Wettability Alteration in Oil-Wet Reservoirs Containing Heavy Oil. *Journal of SPE Reservoir Evaluation & Engineering.* Preprint (to appear). SPE-170034-PA. http://dx.doi.org/10.2118/170034-PA.

Mohammed, M., Babadagli, T. 2013. Efficiency of Solvent Retrieval during Steam-Over-Solvent Injection in Fractured Reservoirs (SOS-FR) Method: Core Scale Experimentation. Presented at SPE Heavy Oil Conference, Calgary, Alberta, Canada. 11–13 June. SPE-165528-MS. http://dx.doi.org/10.2118/165528-MS.

Naderi, K. and Babadagli, T. 2011. Pore-Scale Investigation of Immiscible Displacement Process in Porous Media Under High-Frequency Sound Waves. *J. Fluid Mech*. **680**: 336–360.

Okandan, E. 1977. Improvement of Waterflooding of a Heavy Crude Oil by Addition of Chemicals to the Injection Water. Presented at SPE International Oilfield and Geothermal Chemistry Symposium, San Diego, California, 27–29 June. SPE-6597-MS. http://dx.doi.org/10.2118/6597-MS.

Pathak, V., Babadagli, T. and Edmunds, N.R. 2013. Experimental Investigation of Bitumen Recovery from Fractured Carbonates Using Hot-Solvents. *J. of Canadian Petr. Tech.* **52** (4): 289–295.

Pathak, V., Babadagli, T. and Edmunds, N.R. 2011. Heavy Oil and Bitumen Recovery by Hot Solvent Injection. *J. Petr. Sci. and Eng.* **78**: 637–645.

Pathak, V., Babadagli, T. and Edmunds, N.R. 2012. Mechanics of Heavy Oil and Bitumen Recovery by Hot Solvent Injection *SPE Res. Eval. and Eng.* **15** (2): 182–194.

Risk Reactor Inc. www.riskreactor.com (accessed February 2014).

Seethepalli, A., Adibhatla, B., and Mohanty, K.K. 2004. Wettability Alteration During Surfactant Flooding of Carbonate Reservoirs. Presented at SPE/DOE Symposium on Improved Oil Recovery, Tulsa, Oklahoma, 17–21 April. SPE-89423-MS. http://dx.doi.org/10.2118/89423-MS.

Wei, Y. and Babadagli, T. 2016. Selection of Proper Chemicals to Improve the Performance of Steam Based Thermal Applications in Sands and Carbonate. SPE 181209, 2016 SPE Latin

America and Caribbean Heavy and Extra Heavy Oil Tech. Conf., Lima, Peru, 19–20 October.

| Materials | Density at 25°C (g/cm3) | Viscosity at 25°C (cp) |
|---|---|---|
| Mineral Oil | 0.8390 | 474.3 |
| Heptane | 0.684 | 0.386 |

**Table 3.1—Physical properties of oil and solvent used in these experiments.**

| No. | Chemical Name | Chemical Type | Concentration |
|---|---|---|---|
| 1 | Surfactant A | internal olefin sulfonate (IOS) | 1wt% |
| 2 | Surfactant B | internal olefin sulfonate (IOS) | 1wt% |
| 3 | Surfactant C | internal olefin sulfonate (IOS) | 1wt% |
| 4 | SiO2 | Nanofluid | 1wt% |
| 5 | Al2O3 | Nanofluid | 1wt% |
| 6 | BMIMBF4 | Ionic liquid | 0.75wt % |

**Table 3.2— Types and parameters of selected surfactants.**

| Chemical | Concentration | IFT @25°C (mN/m) |
|---|---|---|
| SiO2 | 1%wt | 3.43 |
| Al2O3 | 0.75%wt | 4.1 |
| Ionic liquid | 1%wt | 7.27 |

**Table 3.3—IFT values of selected surfactant.**

| Exp. No. | Oil Type | Surfactant Type | Injection Rate | Mass Rate |
|---|---|---|---|---|
| 1 | MO | Surfactant A | 0.06ml/hr | 1%wt |
| 2 | MO | Surfactant B | 0.06ml/hr | 1%wt |
| 3 | MO | Surfactant C | 0.06ml/hr | 1%wt |
| 4 | MO | Ionic liquid | 0.06ml/hr | 1%wt |
| 5 | MO | Silicon oxide | 0.06ml/hr | 1%wt |
| 6 | MO | Aluminum oxide | 0.06ml/hr | 0.75%wt |

**Table 3.4—Parameters designed for the microfluidic experiments to assess the Surfactants.**


**Fig. 3.1—Schematic of 2-D visualization set-up.**

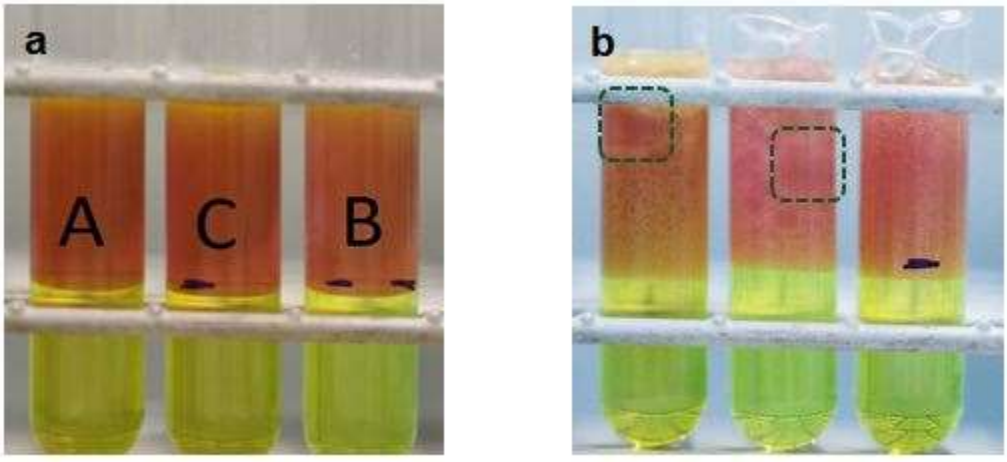


**Fig. 3.2—Microemulsion tests of sulfonate chemicals:a) initial stage; b) after three days.**

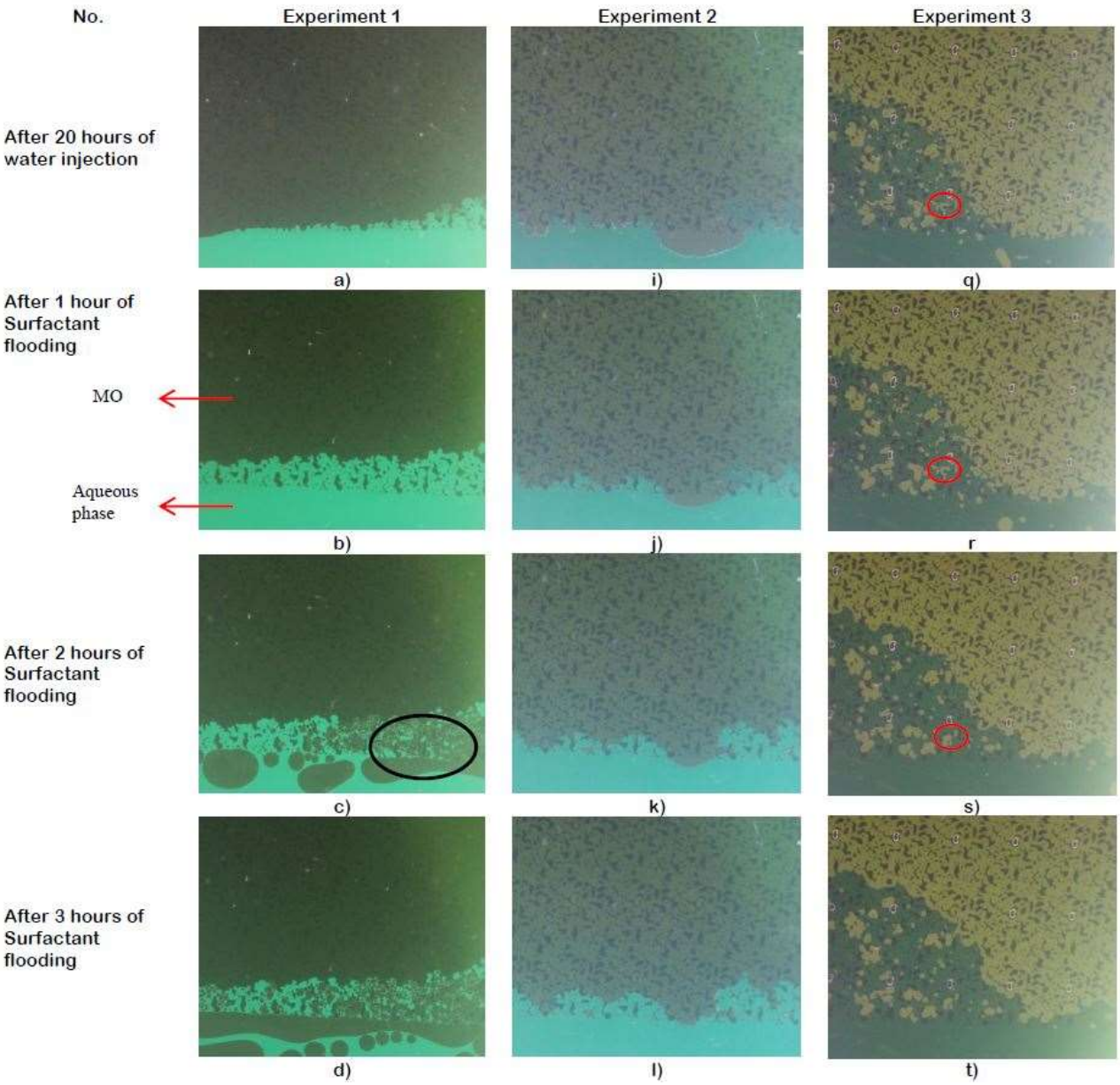
No.
Experiment 1
Experiment 2
Experiment 3
After 20 hours of water injection
a)
i)
q)
After 1 hour of Surfactant flooding
MO
Aqueous phase
b)
j)
r
After 2 hours of Surfactant flooding
c)
k)
s)
After 3 hours of Surfactant flooding
d)
l)
t)

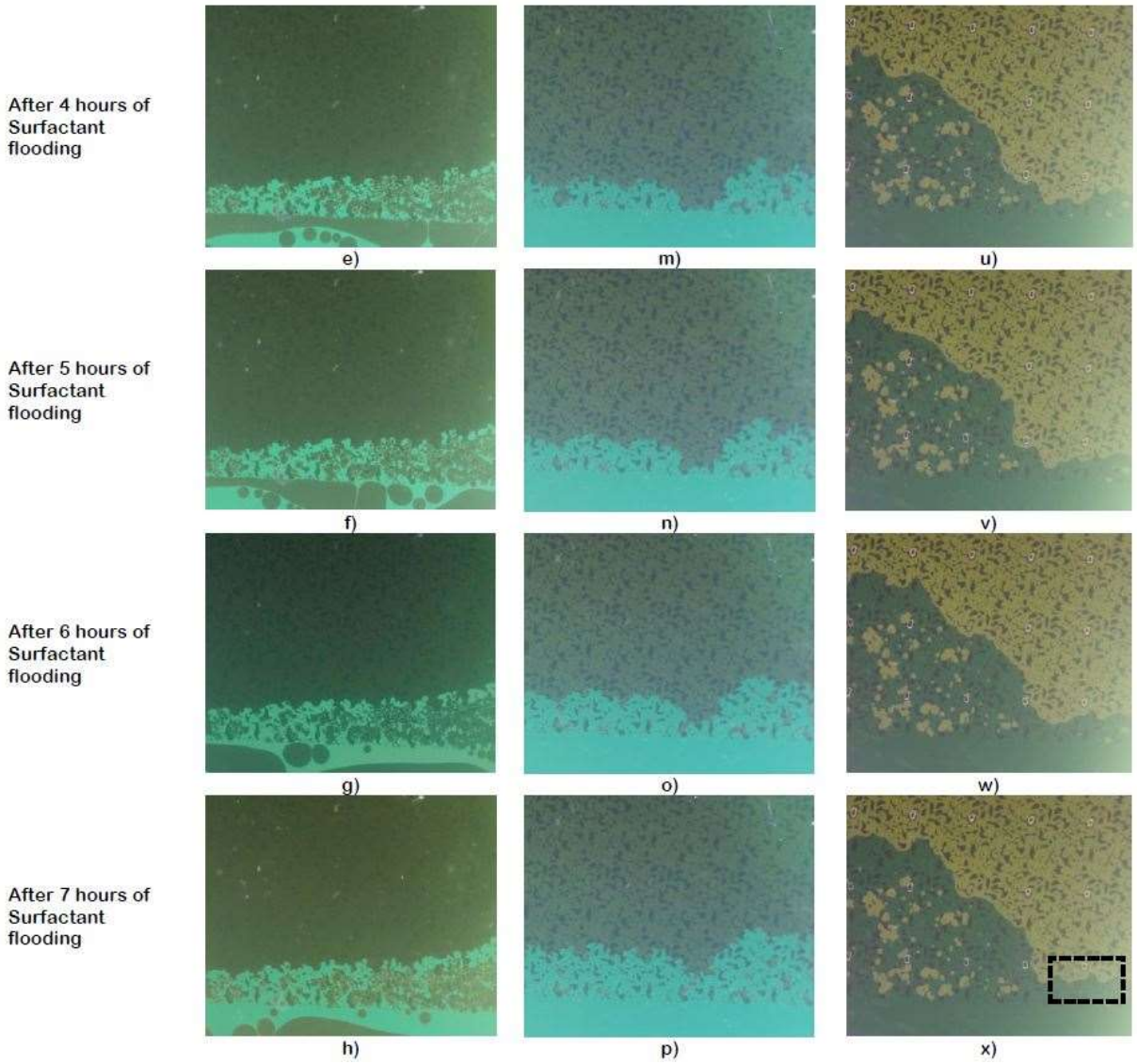


**Fig. 3.3—Visualization of surfactant flooding process: a)-h)-surfactant A; i)-p)-surfactant B; q)-x)-surfactant C.**

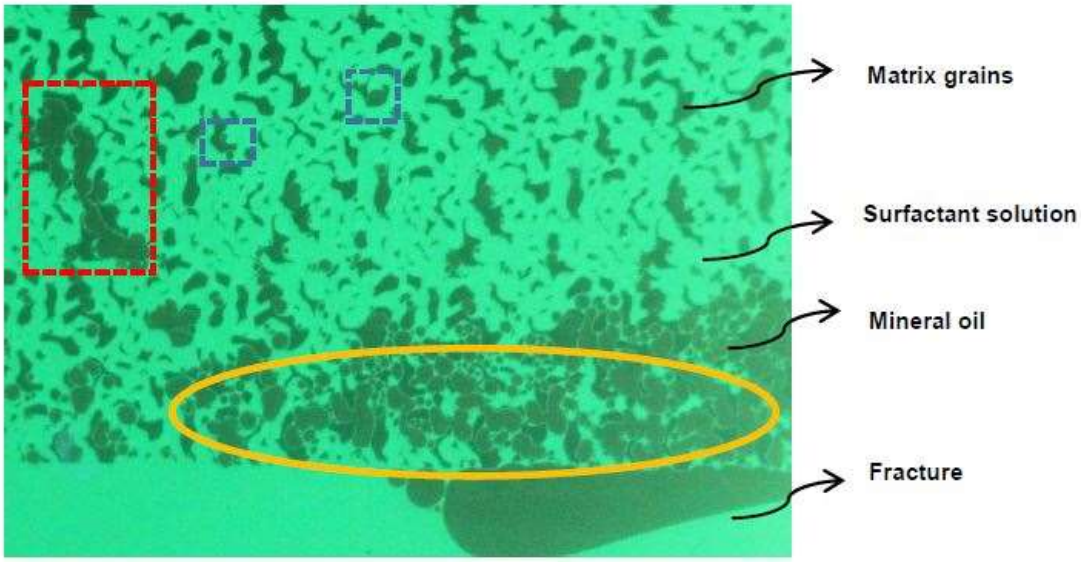


**Fig. 3.4—Phase distribution in pores after surfactant flooding in Experiment 1.**

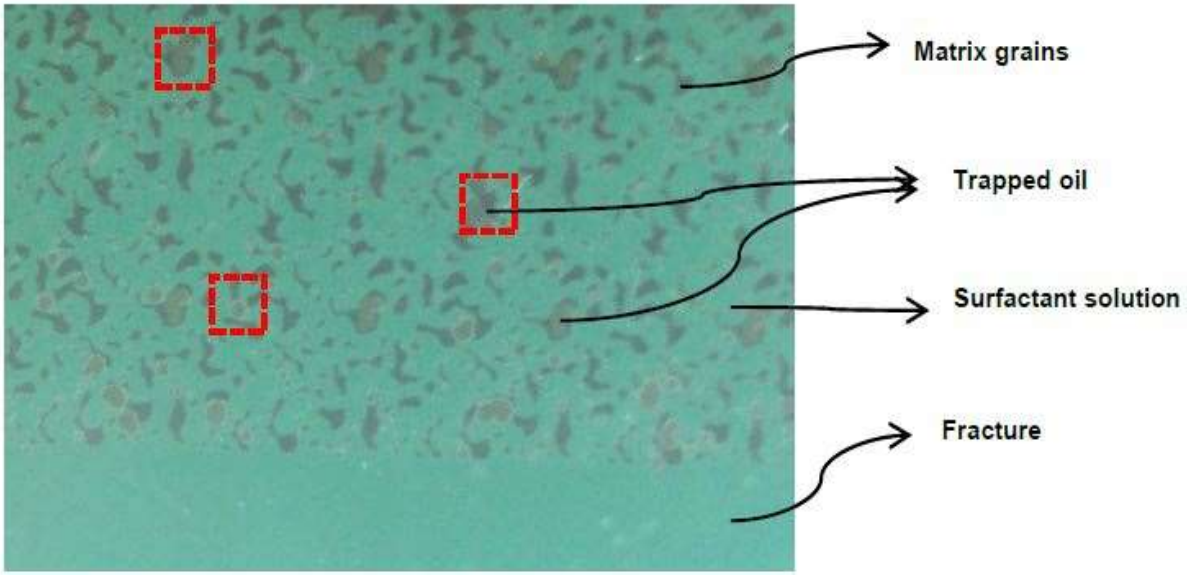


**Fig. 3.5—Phase distribution in pores after surfactant flooding in Experiment 2.**

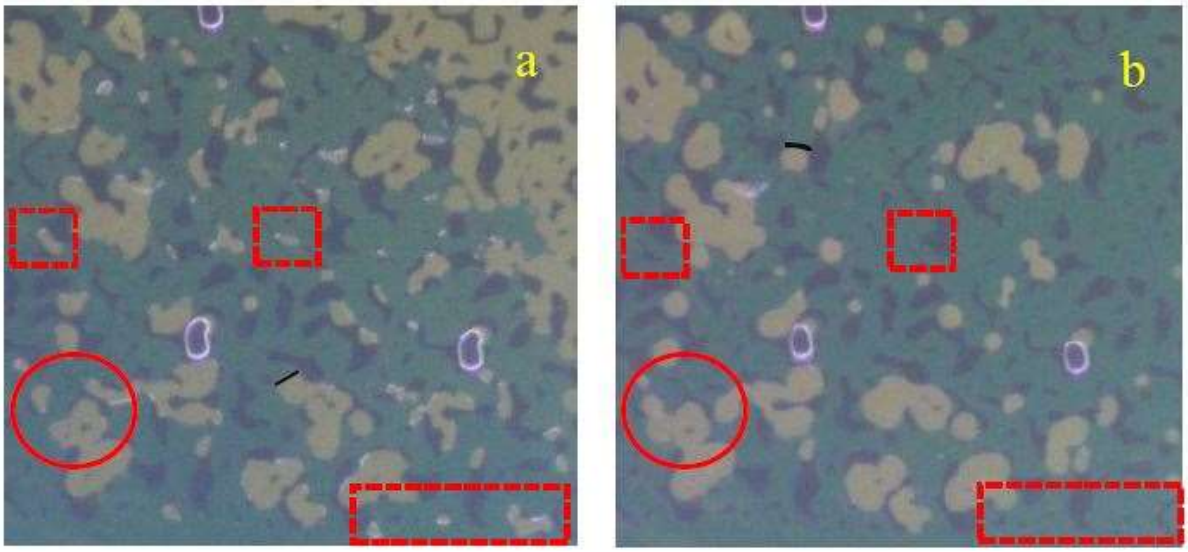


**Fig. 3.6—Close-up images of phase distribution after Experiment 3: a) after water displacement; b) after surfactant flooding, saturation of residual oil = 17.15%.**

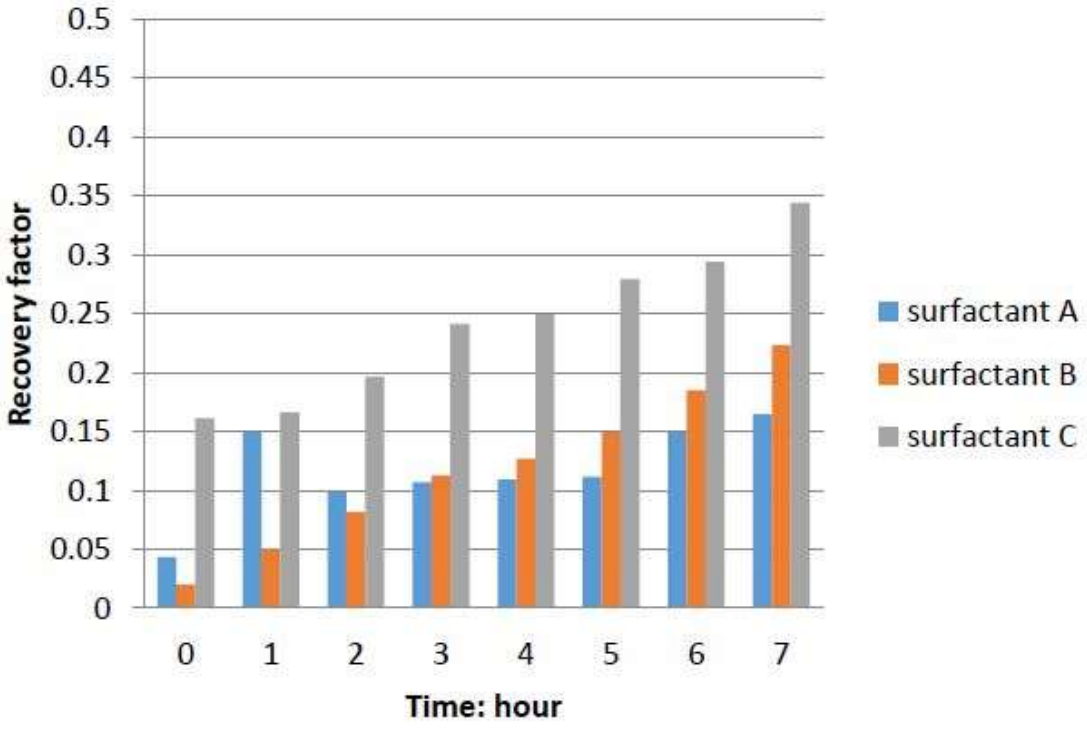


**Fig. 3.7—Recovery factor of the flooding process at intervals of time.**

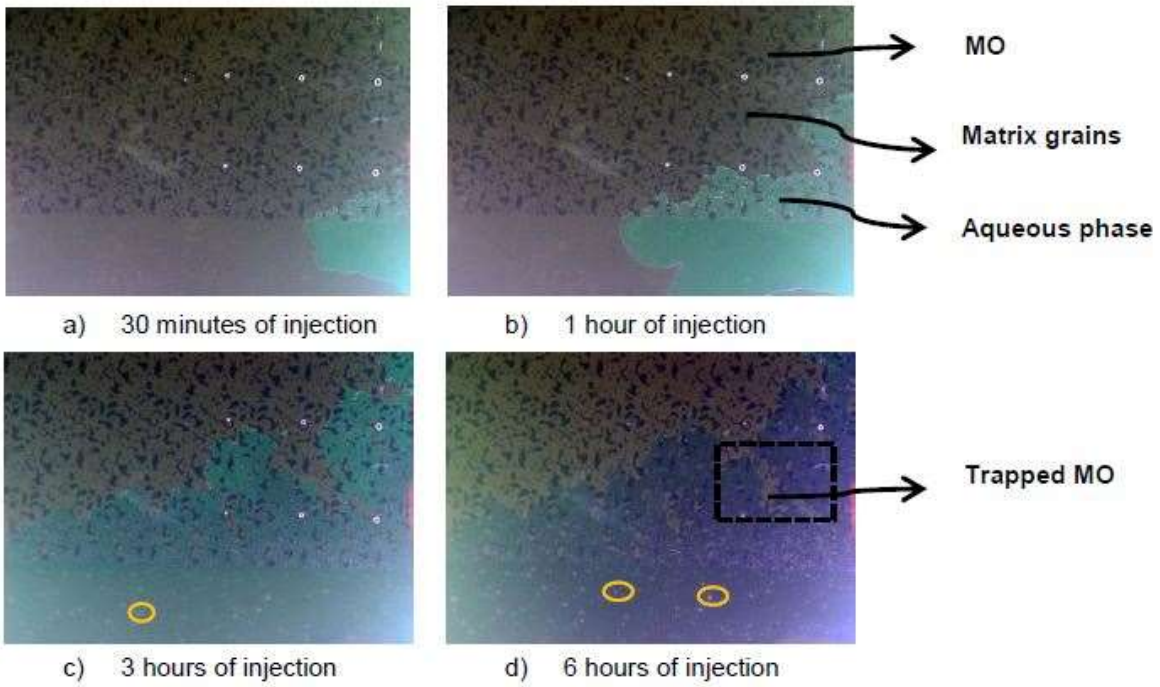


**Fig. 3.8—Ionic liquid flooding process: 1%wt concentration and 0.001ml/min.**

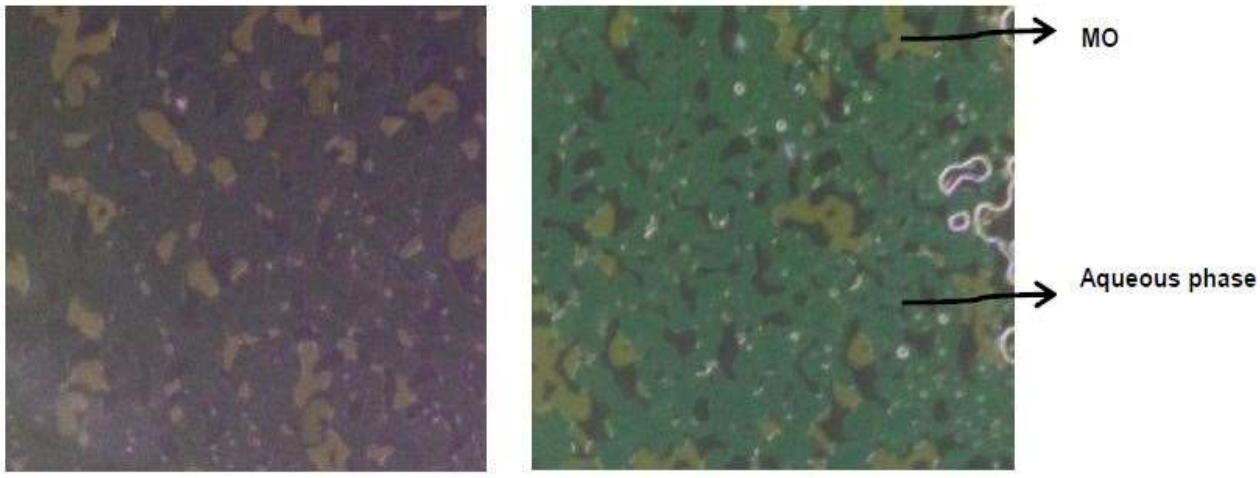


**Fig. 3.9—Residual oil distribution of experiments using a) ionic liquid (residual oil saturation = 15.05%); b) silicon dioxide (residual oil saturation = 22.2%).**

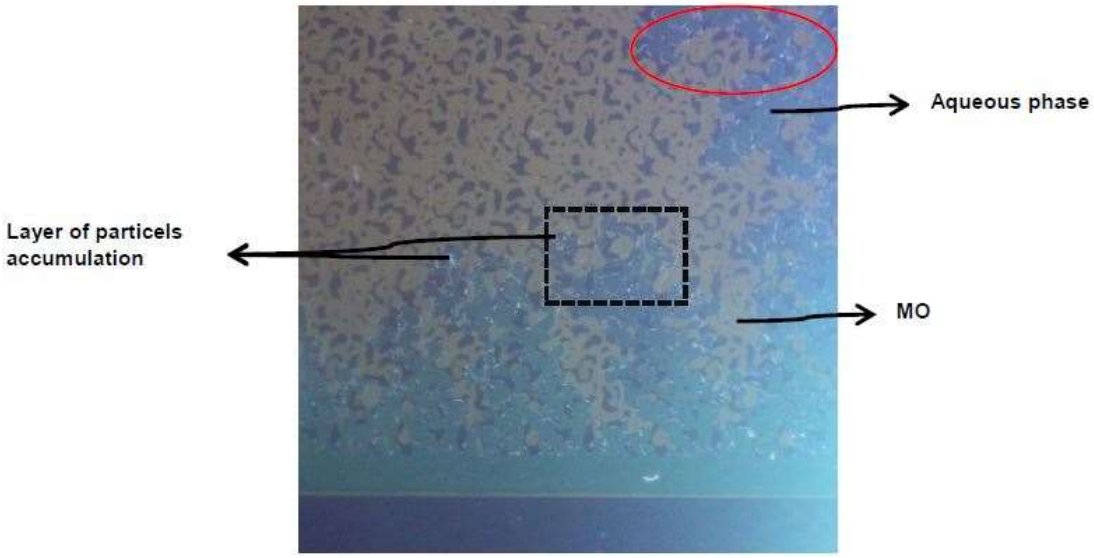


**Fig. 3.10—Phase distribution after 20 hours of injection using $Al_2O_3$ solution (0.75wt%).**

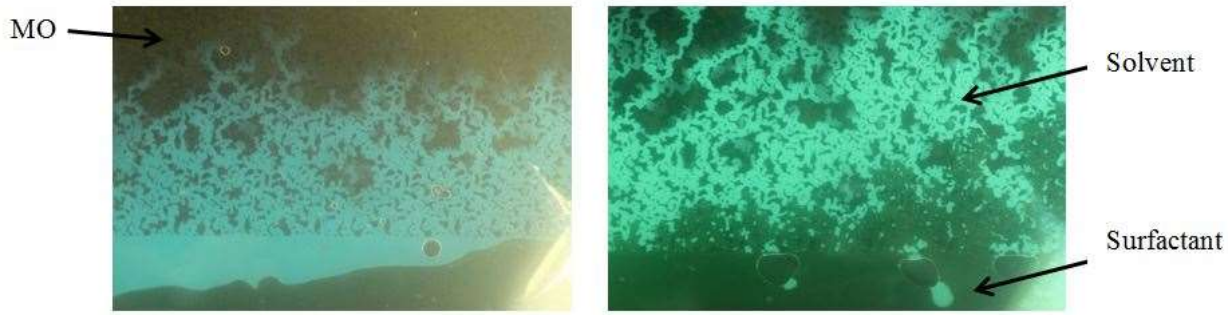


**Fig. 3.11— Sufactant injection after pre-solvent stage (heptane), MO: mineral oil.**

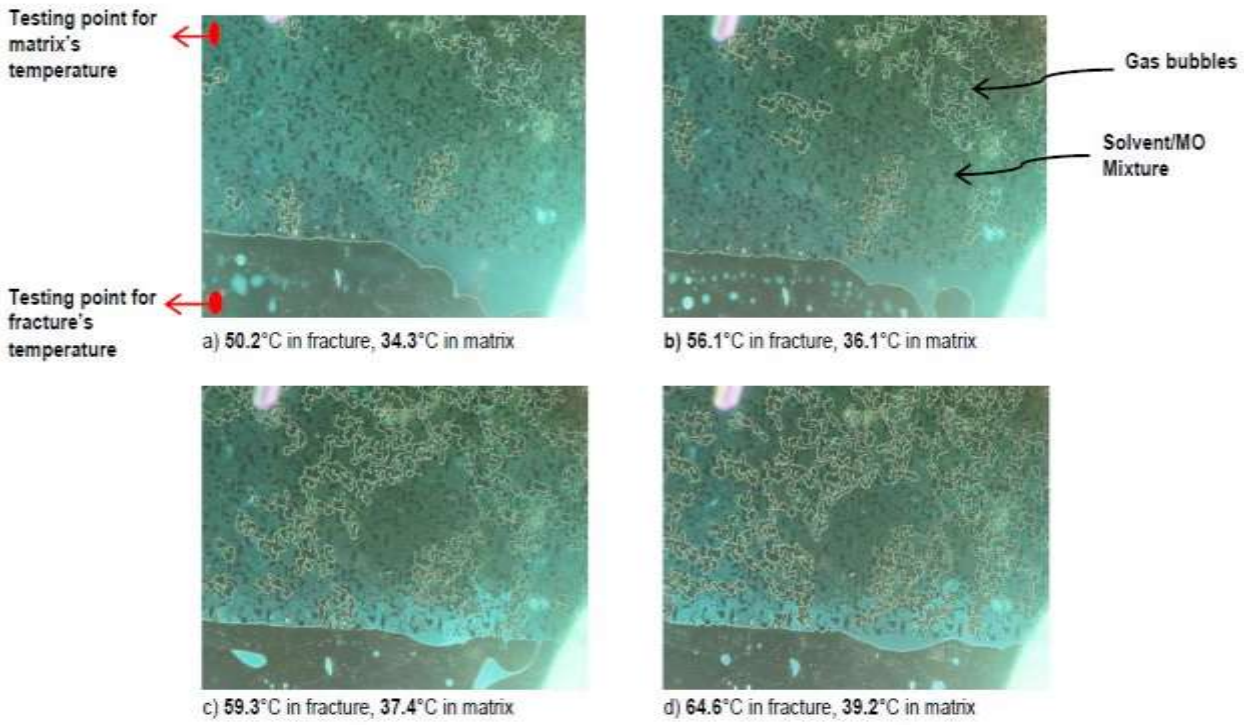


**Fig. 3.12—Solvent boiling and retrieval process (oil wet, fracture heating and heptane).**

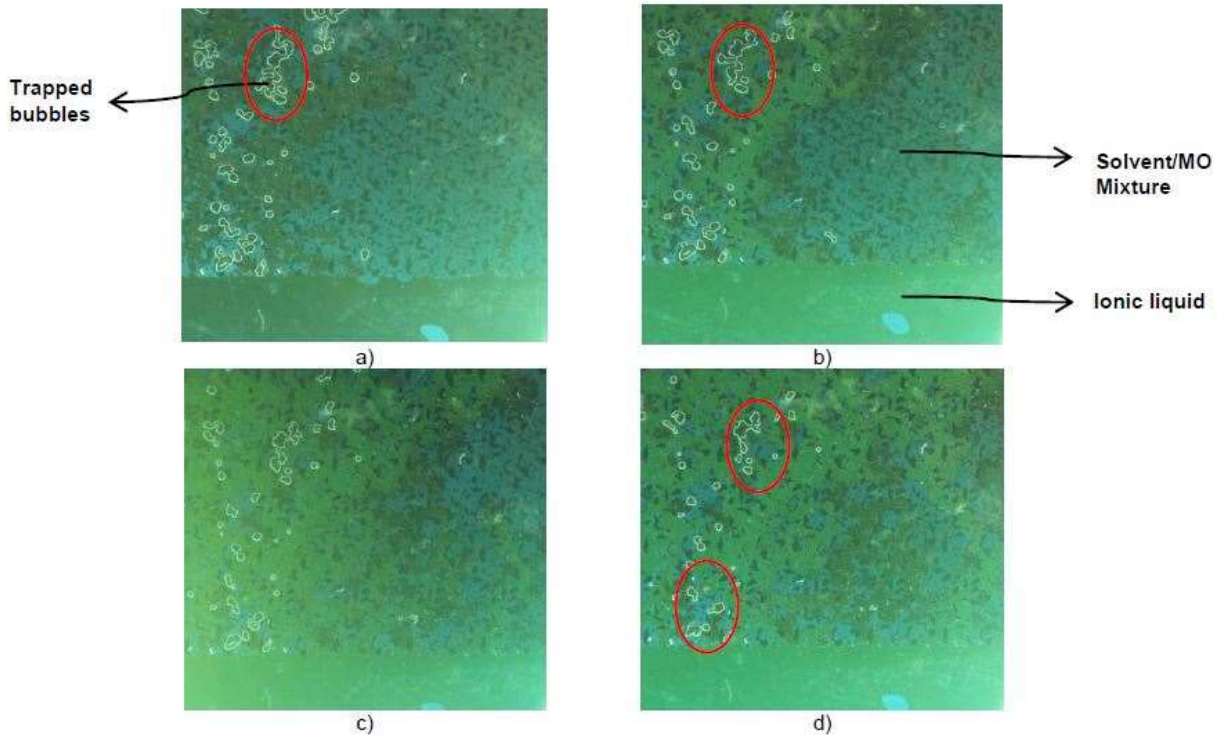


**Fig. 3.13—Chemical flooding aided solvent retrieval process (oil wet, 1wt%ionic liquid).**

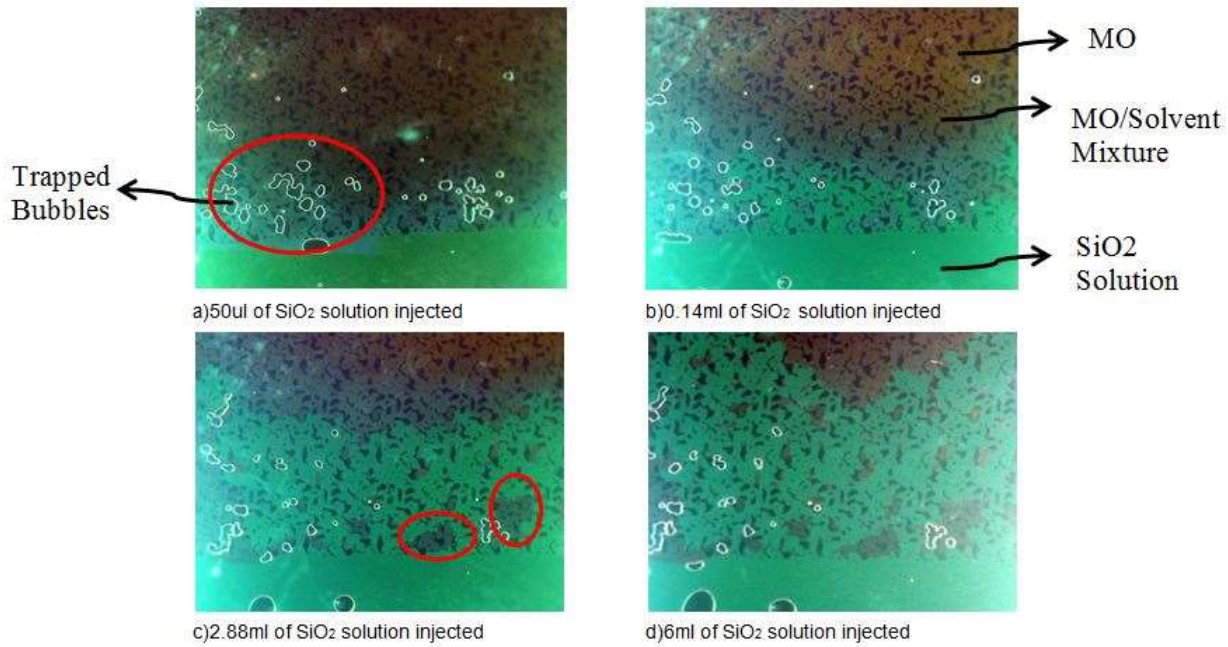


**Fig. 3.14— Chemical flooding aided solvent retrieval process (oil wet, 1wt% silicon dioxide solution).**

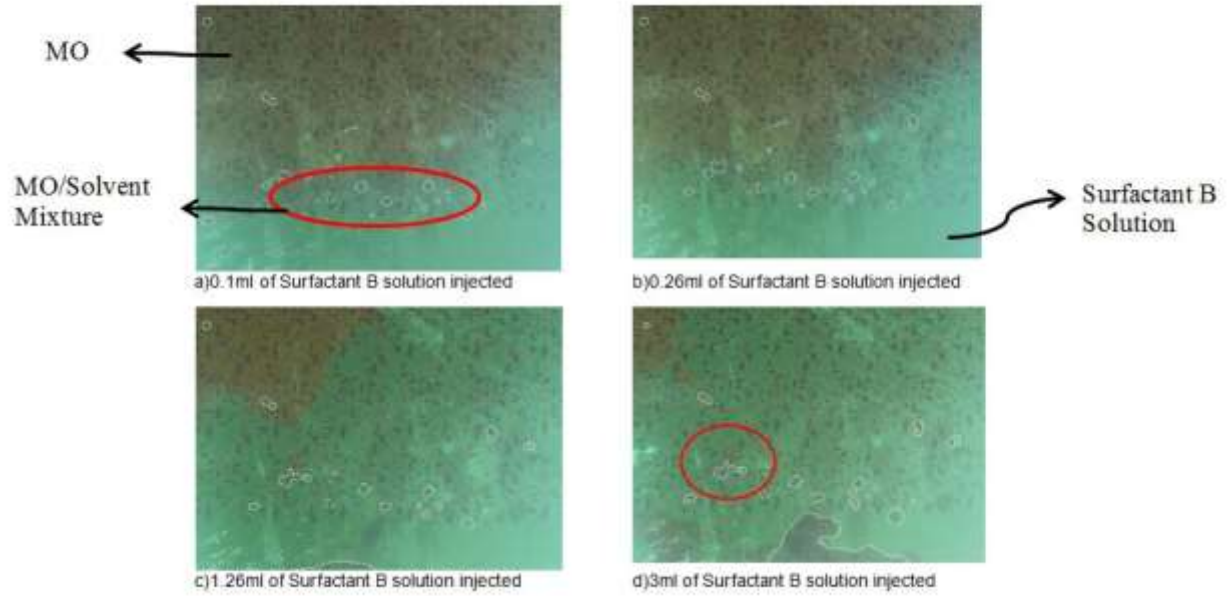


**Fig. 3.15— Chemical flooding aided solvent retrieval process (oil wet, 1wt% Surfactant B solution).**

# CHAPTER 4: CONCLUSIONS AND CONTRIBUTIONS

## 4.1 Conclusions and Contributions

With the development of the solvent aided technologies, the requirement of retrieving expensive solvent back has gradually grasped our attention. Thermal methods and chemical injection were proposed to achieve solvent retrieval effectively, especially in complex reservoirs with heterogeneity. Previous research mainly focused on core-scale experiments to understand the process and gain data to optimize the parameters related to these technologies. Pore scale investigation is needed to give us a clear understanding about these processes for further simulation and optimization studies.

The major contributions from this thesis as well as the limitations of this research are listed below:

- High resolution 2-D images of the solvent retrieval process dealing with heating are obtained to understand the mechanism of the designed solvent vaporization at variable temperatures. When the liquid phase is bonded by other fluids or solid matrix in pores, then the fluid's interface is curved and there is a pressure difference across the curve, which further affects the phase equilibrium. The phase equilibrium under this kind of condition will be different from the flat interface case. In these experiments, the solvent started to form bubbles at low temperature than boiling point temperature under bulk condition. Furthermore, the temperature required under oil-wet case is even lower than water-wet case in our designed porous micromodel due to the change in the interfacial tension, which is in line with the Thomson equation (Eq. 1).

- Different heating patterns are designed and compared. It is shown that the high heating rate leads to quick boiling without enough time to allow bubbles to develop into smaller

pores and throats. There are more obvious trapped solvent in liquid phase by the network of the bubbles. Different oil types and solvent types are chosen in these experiments. Oil viscosity is shown to have no obvious effect on the temperature starting to boil. Different solvents have similar phenomena in pores but a slight temperature difference according to their own physical properties.

- Glass-tube experiments are designed to understand the micro-emulsion behaviour of the selected surfactants with the heavy-oil used. Using this information and micromodel visual experiments, the most efficient chemical for heavy-oil and solvent recovery in fractured system is determined.

- The heat provided to the reservoirs to retrieve the solvent back also diluted the oil at the same time. It is better to produce the additional oil and more solvent back so as to not wasting the energy. It is shown that the final recovery is better when solvent aided process is applied rather than pure water injection or surfactant injection.

- Due to the fragility of the glass model, pressure applied to saturate oil is limited. Therefore, the oil viscosity is limited to 600cp (at 20°C). This can be increased using stronger materials and design. Also, this work focuses on the temperature effect and visualization. The highest temperature applied was 80°C. For high temperature experiments, glass type and proper material to frame it should be used. To totally understand the complex mechanism of this process, the high pressure system is also needed to consider the pressure change (Kelvin effect). This requires pressure resistance (framed) models.